Review Article

Nuru-Deen Jaji, Muhammad Bisyrul Hafi Othman*, Hooi Ling Lee, Mohd Hazwan Hussin, Hazizan Md Akil, Zulkifli Merican Aljunid Merican, and Mohd Firdaus Omar

Polyimide–nickel nanocomposites fabrication, properties, and applications: A review

https://doi.org/10.1515/rams-2023-0113
received January 31, 2023; accepted August 18, 2023

Abstract: Taking inspiration from many published review articles in respect of polyimide–nickel nanocomposites (PINiNCs), this article is written to highlight the significant effect of reinforcing and/or blending nickel nanoparticles (NiNPs) with the different constituents of polyimide monomers to increase various properties (mechanical, thermal, and stability) without sacrificing any of its positive properties. The design and fabrication methodologies of PINiNCs have been critically reported. The recent characterization probing techniques and applications, revealing their advantages and disadvantages are examined in depth. Their diverse applications in multidisciplinary as well as high technological fields and their corresponding properties are extensively documented and summarized in tables. The type of NiNPs and the detailed fabrication techniques of PINiNCs together with their advantages and disadvantages were documented. The combination between this reported fabrication technique and enhanced properties also inspires and broadens the reader's view to understand the basic principle of structure properties relationship of PINiNCs. This review also screens the properties and current application of PINiNCs in the field of lithography technology, biomedical, electrode technology, membrane, dielectric materials, and light emitting diode technology. The main findings are focused on the strategies to fabricate novel PINiNCs. Various modern cutting-edge characterization technologies for PINiNCs have been emphasized. The industrial applications of PINiNCs have been thoroughly reviewed to develop a complete reference material on PINiNCs.

Keywords: polyimide, nickel nanoparticles, nanocomposite, fabrication, characterization, applications

*** Corresponding author: Muhammad Bisyrul Hafi Othman**, School of Chemical Sciences, Universiti Sains Malaysia, Gelugor, 11800 Penang, Malaysia, e-mail: bisyrul@usm.my, tel: +60 46534032; fax: +60 46574854
Nuru-Deen Jaji: School of Chemical Sciences, Universiti Sains Malaysia, Gelugor, 11800 Penang, Malaysia; Federal College of Education Technical, PMB 060, Gombe, Gombe State, Nigeria
Hooi Ling Lee: Nanomaterials Research Group, School of Chemical Sciences, Universiti Sains Malaysia, 11800 Gelugor, Penang, Malaysia
Mohd Hazwan Hussin: School of Chemical Sciences, Universiti Sains Malaysia, Gelugor, 11800 Penang, Malaysia
Hazizan Md Akil: School of Materials and Minerals Resources Engineering, Engineering Campus, Universiti Sains Malaysia, 14300 Nibong Tebal, Pulau Pinang, Malaysia
Zulkifli Merican Aljunid Merican: Department of Fundamental & Applied Sciences, Universiti Teknologi PETRONAS, 32610 Seri Iskandar, Perak, Malaysia; Institute of Contaminant Management, Universiti Teknologi PETRONAS, 32610 Seri Iskandar, Perak Darul Ridzuan, Malaysia
Mohd Firdaus Omar: Faculty of Chemical Engineering & Technology, University Malaysia Perlis (UniMAP), 02600, Arau, Perlis, Malaysia; Centre of Excellence Geopolymer and Green Technology (CEGeoGTech), Universiti Malaysia Perlis 02600, Arau, Perlis, Malaysia

1 Introduction

Since 1960–2018, the total global production of composites was 288 metric tons at the rate of 0.2 metric tons annually and estimated to be 199,000 tons by 2022 [1]. The most prominent usage was recognized in promising research area of electronic and aerospace engineering products including circuit boards, radiation resistant components, coatings, optoelectronic, and magnetic ingredients. Additionally, suitable for wide range applications such as coatings, catalysis, radiation, magnetic devices as well as biomedical applications. This is because (1) they are lighter than conventional composites because high degrees of stiffness and strength are realized with far less high-density material, (2) their barrier properties are improved compared with the neat polymer, (3) their mechanical and thermal properties are potentially superior, and (4) exhibit excellent flammability properties and increased biodegradability of biodegradable polymers [2], polymers are used in sliding couples against metallic materials [3]. Among the inorganic nanofillers extensively used are gold [4], iron [5], nickel [6], magnesium [7], silver [8], and titanium [9].

Nickel nanoparticles (NiNPs) have received much attention due to their excellent magnetic, chemical, and physical properties [10]. In view of their unique properties, they have the potential for applications in battery manufacture, catalysis [11], smart textile, nanotube-printing ink [12], optical switches and field modulated gratings, adsorption of dyes, and immobilization of molecules through magnetic force [13]. Elsewhere, reports indicate that NiNPs are applicable in super capacitors with high specific capacitance [14]. They are used as an electrocatalyst in the oxidation of methanol and water with high catalytic activity compared to platinum counter electrodes [15]. In energy storage they are employed as an alternative to expensive platinum counter electrode [16]. In neuromorphic computing NiNPs serve as hardware. NiNPs are identified in the catalysis of Suzuki–Miyaura cross-coupling reactions [17]. In view of the relatively small size of NiNPs, they are used in applications such as nanoelectronics, catalysis, and hydrogen storage [18]. Nanocomposites containing nickel function as the anode in electrochemical reactions with enhanced electrical conductivity leading to outstanding fast kinetics [12]. Nickel metal exhibits variable magnetic susceptibility at room temperature. However, the magnetic properties are heavily affected by the size, shape, and morphology of the NiNPs [19]. The exclusive properties of nanomaterials give them superiority over bulk materials; therefore, NiNPs have broader application prospects [20]. Polyimide (PI) matrix filled with metal nanoparticles such as nickel, silver, and gold exhibit good heat conductivity with subsequent advanced material applications. PIs containing nickel in its matrix are of great interest in nanotechnology and achieve excellent properties due to organic and inorganic synergic effects [21]. They have been specifically reported as being used in heterogeneous catalysis [22], electrochemical sensing of glucose [23], electronic packaging [24], biochemical reactions [25], thermal insulation [26], photocatalysis [27], antibacterial activity [28], dielectric applications [29], electromagnetic shielding [30], microwave absorption [31], biomedical applications [32], improvement of tensile properties for bearing applied force [33], improved electrical conductivity [34], supercapacitors [35], selective capture of mono-phosphopeptides [36], improved electrical conductivity [37], removal of lead from aqueous solution [38], enhancement of electrochromic efficiency [39], improved electrochemical activity [21], magnetic resonance imaging technologies [40], gas separation [41], and as an effective diffusion barrier [42].

PIs exhibit high thermal stability, excellent mechanical strength, superior chemical and radiation resistance [43], high adhesion properties, ability to form good films, and low dielectric constant [44]. Hence PIs provide an excellent matrix for the fabrication of nanocomposite materials with good thermal and chemical stability [45]. However, the poor conducting properties of PIs limit their applications in electrical and electrochemical devices. Moreover, due to poor thermal conductivity PIs cannot meet the requirement of fast heat conduction for advanced electronic devices. The effective strategy to improve thermal transport is by introducing thermally conductive fillers such as metallic nanoparticles [46], graphene-based materials [47], and ceramic materials to the PI matrix [48]. In high technology applications, failure prevention in seafloor pipeline can be prevented by grouting the annulus of the double-wall pipeline with polymers [49], 4D applications [50], and glass fiber-reinforced nanocomposites [51]. Therefore, the methodology of fabrication, characterization, and applications of PI–metal nanocomposite materials with good thermal conductivity becomes highly imperative.

A wide range of PIs have been obtained by changing the chemical structure of the dianhydrides and diamine monomer fragments of macromolecules with different structure and properties. The classification of PIs based on chemical structure and physical properties are summarized in Table 1.

PI matrix is an emerging type of high-performance material with remarkable thermal and dielectric properties [56], medical applications in extreme environment and high temperatures [57], as well as excellent mechanical properties of high strength and high modulus [58]. PI matrix has attracted significant attention in the field of advanced composite for aviation and aerospace applications owing to its satisfactory combination of excellent physical and chemical properties. PI matrix can be used in a wide range of temperatures, and they match well with high temperatures and pressures applied in the processing of high-performance resins.

In the present work on polyimide–nickel nanocomposites (PINiNCs), we herein critically report various preparation methodologies of PINiNCs design and fabrication,

Table 1: Summary of the classification of PIs based on their chemical structure and physical properties

PI category	Chemical properties	Physical properties	Ref.
Group A	Aromatic imides cyclic	Non-softening, brittle, heat resistance	[52]
Group B	Hinges in dianhydride	Non-softening rigid with some softening	[53]
Group C	Hinges in diamine	Rigid, strong, elastic	[54]
Group D	Hinges in diamine and dianhydride	Elastic with clear region of softening and melting	[55]

recent characterization techniques and applications, respectively, revealing their advantages and disadvantages. The diverse applications in multidisciplinary fields and corresponding properties are highlighted as well as summarized in tables. This work should provide inspiration for the preparation, characterization, and applications of PINiNCs materials. Moreover, it highlights their current engineering and industrial applications.

2 Types of PINiNCs

2.1 PINiNCs

The historical background of polymer blends indicates that the first patent polymer blend was a mixture of natural rubber, with gutta percha patented by Alexander Parkes in 1846. The first man-made polymer, nitrocellulose was prepared by Braconnot in 1833. The resin was commercialized in 1868. The first patent on blends of two synthetic polymers was granted in 1928 for poly(vinylchloride)/poly(vinylacetate) latex blending. Within the interceding 65 years, the polymer blend patent literature grew at an exponential rate; since 1983 the annual output has doubled, to exceed 3,000 patents per year in 1993 [59]. In the year 2018, the annual global production of polymer composites reached 11.4 metric tons. In 2010, the global production of polymer composites was 51 metric tons, in 2020 it became 160 metric tons and is estimated to be 199 metric tons by 2022 [1]. In the current era, advanced polyimide nanocomposite materials play a major role in the fields of medical science, aerospace, and power sector [60].

Several techniques for the preparation of PINiNCs abound in literature. The development of new class of PINiNCs is motivated by the achievement of performance improvement, ease of processability, and cost effectiveness. The topical issues to be addressed depend upon the intended applications. Such issues may include chemical reactivity, thermal stability, mechanical properties, durability, and electrical as well as electrochemical properties [61]. In the last decade, various techniques have been reported for the preparation of PINiNCs. The surface metallization of Ni on PI matrix is shown in Figure 1.

These techniques include, solution blending and casting technique [41], magnetic field solvent casting [62], ion exchange technique [44], gamma radiolytic method [37], fused filament fabrication [63], electrochemical oxidative polymerization [21], surface metallization of PI technique [42], and polyol method [39]. A method for fabricating highly dispersed metal nanoparticles inside PI resins was proposed by Nawafune *et al.* [64]. A summary of techniques for fabrication of PI–nickel composites is presented in Table 2.

2.2 Polyimide–nickel oxide (NiO) nanocomposites

NiO nanoparticles have generated great interest due to their wide-ranging applications in diverse fields such as catalysis [73], fuel cell electrodes [74], electrochromic films [75], gas sensors [76], smart windows [77], and lithium-ion batteries [78]. These types of hybrid composites acquire the functionalities of metal nanoparticles as well as the

Table 2: Techniques for fabrication of PINiNCs

PI monomer	Synthesis technique	Nickel component	Ref.
PMDA/ODA	Chemical vapor	Ni foam	[65]
ODA/PMDA	Electroless plating	$NiSO_4·6H_2O$	[66]
PMDA/ODA	Electrochemical	Ni oxide	[67]
ODA/PMDA	Flash evaporation	Cu–Al–Ni–Mn	[68]
PMDA/ODA	Electroless deposition	Ni nanoparticles	[42]
PMDA/ODA	Ion exchange	Ni nanofilm	[69]
BPDA/BAPP	Ion exchange	Ni ions	[70]
PMDA/ODA	Electrospun	Ni nanoparticles	[71]
ODA/PMDA	Electroless plating	Ni coatings	[72]

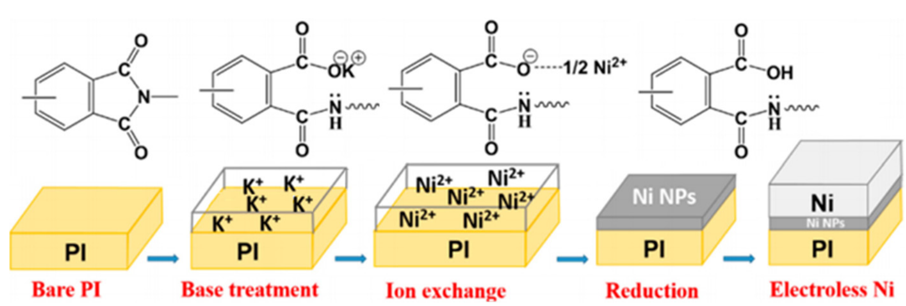

Figure 1: Scheme representing the metallization of Ni on PI film [42].

advantages of polymeric materials such as thermal stability, conformity, and flexibility [79]. Figure 2 presents a typical fabrication of PI/NiO composite.

Novel ferromagnetic PI NiO nanocomposites have been developed by many research groups by dispersing NiO nanoparticles into PI matrix. Table 3 summarizes the fabrication of various PI NiO nanocomposites.

2.3 PI nickel–graphene nanocomposites

PI nickel–graphene nanocomposites have been reported to exhibit high electrical conductivity and actuation performance [84].

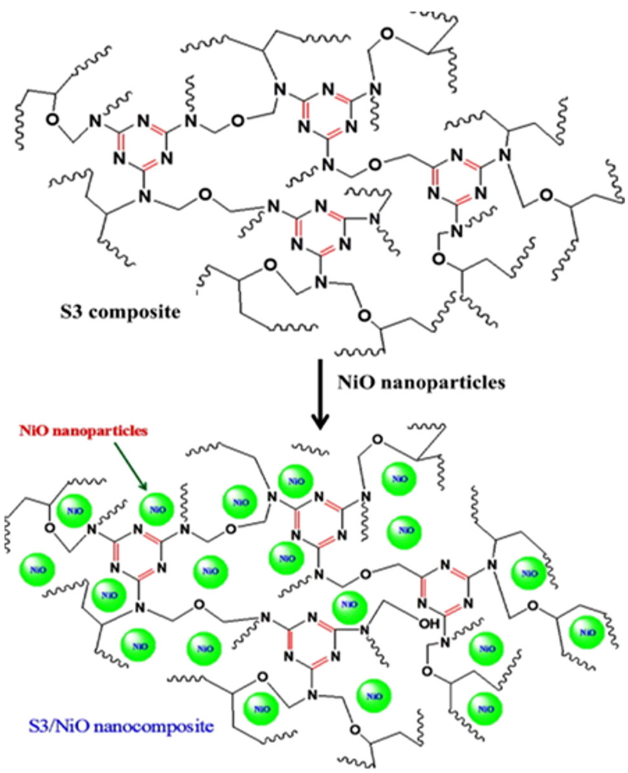

Figure 2: Typical representation of PI/NiO composite fabrication route [80].

The choice of the composite fabrication technique depends on the desired warp including polymer molecular weight, polarity, polymer functional groups as well as the method for graphene functionalization [85]. The multi-component nanocomposite exhibits the characteristics of each component as well as new physical effects due to interactions among the three components. Graphene is a mono-atomic thin layer of carbon atoms connected with σ bonds and a shared π electron cloud forming a honeycomb-like structure of benzene rings [86]. Figure 3 shows stages in the development of PI nickel–graphene thin films.

The thermal conductivity of single layer graphene is reported in the range of 2,500–4,500 $W \cdot m^{-1} \cdot K^{-1}$ [88]. A graphene monolayer has high transparency as well as excellent electrical conductivity. Therefore, the combination of PI with NiNPs and graphene yields multifunctional material with enhanced mechanical, thermal, and electrical conductivity. The research group of Yoonessi *et al.* [62] reported extensively on the fabrication of PI nickel–graphene nanocomposites with outlined potential applications. Table 4 presents the PI matrix and preparation techniques.

Table 4 shows various properties enhanced in the nanocomposites fabricated from PIs, graphene, and nickel nanomaterials. These properties include electrical conductivity of the nanocomposites, enhancement of anticorrosion properties, improved electrochemical activity, excellent mechanical properties, and dielectric properties.

2.4 PI nickel/metal complex nanocomposites

The preparation of nickel complex nanocomposites on PI matrixes have been reported in literature such as PI/copper–nickel ferrite composites [29], Ti–Ni–Cu thin film formed on PI [92], polyethylenes prepared by amine–imine nickel, palladium complexes [93], Ni–Ti–PI composites prepared using thermal imidization technique [94], nickel and palladium complexes with fluorinated alkyl substituted α-diimine ligands [95], and complex formation of polyethyleneimine with

Table 3: Summary of preparation techniques of PI NiO composites

PI monomers	Preparation technique	Nickel type	Enhanced property	Ref.
ODA/PMDA	Imidization	Ni(II)	Electrochemical	[81]
BTDA/DAPI	Solution casting	NiO	Gas selectivity	[41]
PMDA/ODA	Solution casting	NiO precursors	Electrochemical	[67]
PMDA/ODA	Sol gel	Nickel titanate	Magnetization	[82]
BPADA/BAPP	Solvent casting	Ni graphene	Optoelectronic	[62]
BPADA/BAPP	Dispersion	NiO	Hardness	[80]
PMDA/ODA	Polymerization	Ni–Zn–Fe	Electromagnetic	[83]

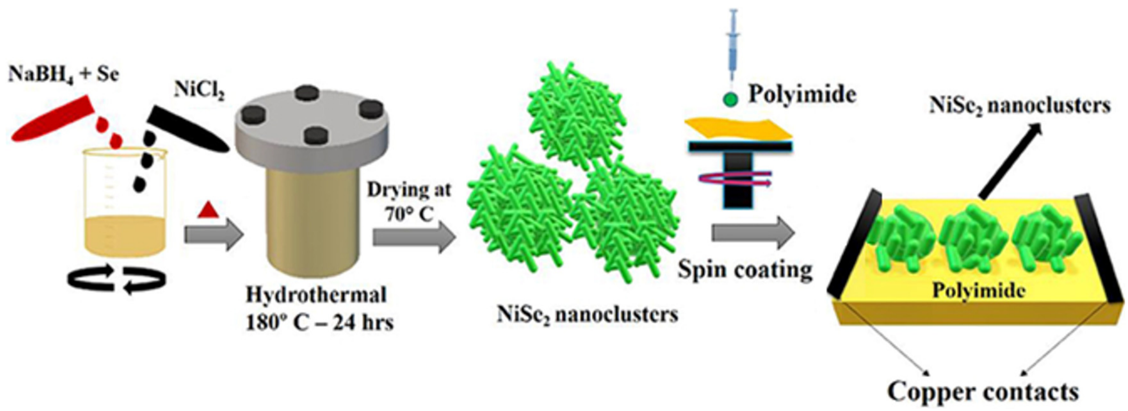

Figure 3: Fabrication of PI nickel–graphene fabric [87].

copper, nickel, and cobalt [96]. The unique properties that arise from the combination of organic and inorganic components in PI nickel complexes are of great importance in advanced materials science research. The PI matrix confers good processability and flexibility, whereas the inorganic component provides electrical, thermal, magnetic, and optical properties [97]. An example of PI nickel/metal complex nanocomposite fabrication is provided in Figure 4. The figure shows the preparation of PI–NiSc nanomaterial.

Nickel complexes incorporated into PI phase impart magnetic properties necessary for a variety of high-performance PI applications, such as photocatalysis, heavy metal absorption, and magnetic imaging [99]. Table 5 provides a summary of preparation techniques, the PI precursor, and enhanced properties of PI nickel complex nanocomposites.

Nanocomposites fabricated by introducing nickel complexes into the PI matrix show excellent catalytic activity, shape-memory actuators, and low dielectric loss. These nanocomposites are good for the development of advanced materials and engineering.

2.5 PI nickel–nonmetal nanocomposites

PI nickel inorganic materials with thermoelectric properties have been widely studied such as PI–NiFe–Ce, PI–Ni–Ti, PI–Ni–Pd, PI–Ni–Co, *etc.* However, PI inorganic composites have several limitations namely poor processability, high cost of production, and environmental pollution due to toxicity. On the contrary, PI–Ni–organic composite thermoelectric materials possess certain advantages such as availability of raw materials, easy applications to fabricate devices, ease of processability, and environmental friendliness. PI–nickel–nonmetal complexes have been fabricated by various techniques as reported in Table 6.

Several preparation techniques have been adopted to produce PI–Ni–nonmetal composite nanomaterials such as wet chemical and electrochemical method, implantation, polymerization, drop-casting, electrophoresis, and conventional copolymerization [110]. A typical route for the fabrication of PI–Ni–nonmetal complex is represented in Figure 5.

3 Fabrications techniques of PINiNCs

3.1 Ultraviolet irradiation

In this technique, metal nanoparticles embedded in PI matrix are simultaneously prepared by gamma rays. The

Table 4: Summary of preparation techniques for PI nickel–graphene composites

PI monomers	Fabrication technique	Nickel type	Enhanced property	Ref.
BPADA/BAPP	Solvent mixing	Ni/graphene	Electrical	[84]
BPADA/BAPP	Solvent mixing	Ni/graphene	Electrical	[62]
PMDA/ODA	Chemical vapor	Ni/graphene	Thermal	[87]
PMDA/PPD	Liquid–solid–solid	Ni(II)	Absorption	[89]
PMDA/ODA	Electrodeposition	NiO/graphene	Electrochemical	[67]
PMDA/ODA	Ion exchange	Ni ions	Structural	[90]
PMDA/ODA	Solution mixing	Ni nanowires	Dielectric	[91]

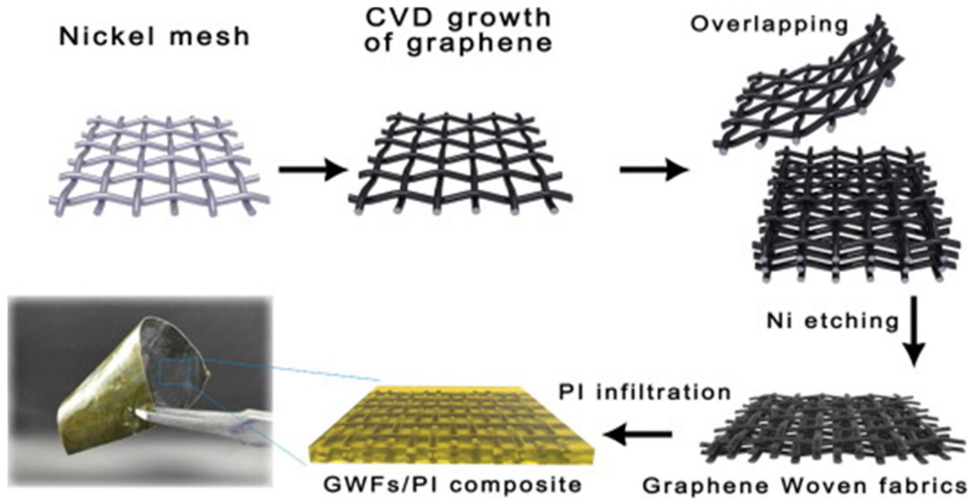

Figure 4: Fabrication of PI–NiSc nanocomposite material [98].

gamma rays induce the oxidation of PI and reduction of nickel ions. This technique provides a clean alternative to chemical methods with subsequent potential in particle size and morphological control by manipulations of parameters such as stabilizing agents, absorbed dose of radiation, dose rate, and the ratio of PI/metal ion precursor [111]. The preparation of nanocomposites by gamma-rays offers two main methodologies for synthesizing nanocomposites in one or two steps. In the first stage, complete nanocomposite can be generated by the combination of monomer or polymer and metallic ions, followed by gamma irradiation in an inert atmosphere. In the second stage, the nuclei, which can be metallic or polymeric, are synthesized first, followed by the shell, which completes the synthesis of the nanocomposite. In some of these steps, either a chemical or gamma-rays process can be used, and in both methodologies, a stabilizer is sometimes required [112]. Figure 6 shows a schematic representation of UV-irradiated surface layer of polymer.

Table 5: Summary of preparation technique, PI precursor, and enhanced properties

PI monomer	Preparation technique	Nickel type	Enhanced properties	Ref.
BAPP/DABA	Imidization	Ni–Cu–Fe–Ce	Dielectric loss	[29]
ODA/PMDA	Sputtering	Ti–Ni–Cu	Memory	[92]
HBPDA/HBPDA	Solution process	NiO	Sensor	[100]
ODA/PMDA	Co-precipitation	Ni complex	Thermal	[101]
PMDA/ODA	Imidization	Ni–Ti	Memory	[94]
PMDA/ODA	Encapsulation	Ni (100)	Adhesion	[102]
NTDA/ODA/ODADS	Electrodeposition	$Ni(OH)_2$	Electrocatalytic	[23]

Table 6: Preparation techniques of PI nickel–nonmetal complex nanocomposites

PI monomers	Fabrication technique	Nickel type	Improved property	Ref.
PTCDA/ODA	Imidization	Ni nanoparticles	Catalytic	[103]
BTDA/ODA	Polymerization	Ni oleate	Catalytic	[104]
ODA/PMDA	Dielectrophoresis	CNT–Ni	Mechanical	[105]
BTDA/ODA	Polymerization	$Ni(HCOO)_2 \cdot H_2O$	Graphitization	[106]
ODA/PMDA	Drop-casting	Ni nano-PETT	Thermoelectric	[107]
BTDA-TDI/MDI	Cross-flow	Ni nanoparticles	Optoelectronic	[108]
BPDA/BPDA	Sputtering	Ni films	Thermoelectric	[109]

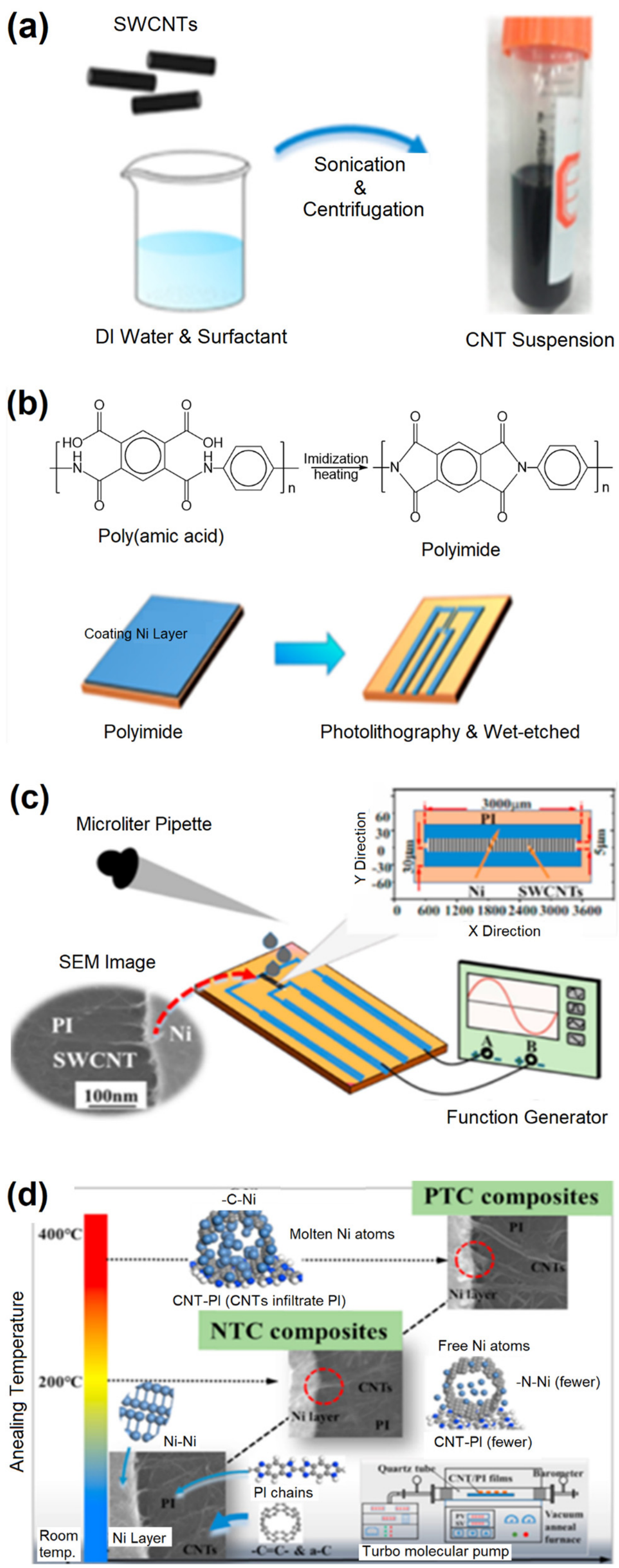

Figure 5: Representation of the fabrication stages in the formation of PI-Ni-CNT film, (a) Preparation of SWCNT suspension, (b) Preparing and patterning of PI-Ni substrate, (c) Formation of SWCNT film, (d) Modified vacuum annealing composite films at various temperatures [105].

Zhang *et al.* [114] prepared NiNP decorated reduced graphene oxide nanocomposites *via* a one-step gamma-ray irradiation induced reduction. Their results showed that NiNPs were uniformly distributed on the surface of the reduced graphene oxide nanosheets. The obtained nanocomposite films showed excellent electromagnetic wave absorption properties. It was therefore concluded that well crystallized NiNPs were deposited on the surface of the reduced graphene oxide nanosheets. Meftah *et al.* [37] synthesized and studied the structural, optical, and electrochemical properties of polyaniline and NiNPs embedded in polyvinyl alcohol film matrix *via* gamma radiolytic technique. The electrical conductivity of the obtained nanocomposites increased with an increase in NiNPs concentration. The ultraviolet–visible spectra showed a blue shift of the characteristic absorption peak of NiNPs due to decrease in particle size with increase in dosage, predisposing the thin nanocomposite films as good catalyst. Some of PI precursors used in ultraviolet techniques are shown in Table 7.

The advantages of UV-irradiation techniques for PI nanocomposites preparation include easy processing, low cost of production, environmental friendliness, valuable functionalities imparted on the PI matrix, and an efficient method to create desirable surface properties [121]. However, certain drawbacks of the techniques include highly specific reaction conditions such as atmosphere of irradiation, wavelength of the irradiated light, and photochemical properties of the polymer.

3.2 *In situ* single stage technique

A wide range of *in situ* techniques for the fabrication of PI metal nanocomposite films have been reported involving thin films casting from a mixture of polymer and intended metal nanoparticles [122]. A prominent *in situ* approach involves the casting of thin films from a mixture of polymer and intended metal nanoparticles. These techniques entail the concurrent *in situ* fabrication of metal nanoparticles and polymer resulting in composite material from which the thin films are developed [123]. In another approach the monomer units are set to polymerize and encapsulate the tailored metal nanoparticles into the polymer matrix. Alternatively, appropriate precursors are employed to generate metal nanoparticles within the polymer matrix [124]. A typical *in situ* procedure for the fabrication of PI metal composites is shown in Figure 7. In the figure, PINiNCs prepared by *in situ* techniques including single step, vapor deposition, and *in situ* encapsulation are presented with nickel

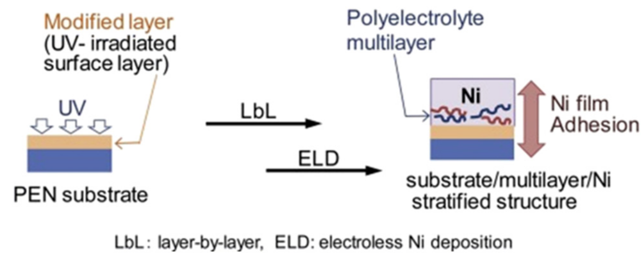

Figure 6: Scheme of UV-irradiated nickel modification of polymer layer [113].

Table 7: Summary of ultraviolet techniques for the fabrication of PI nickel composites

PI monomers	Fabrication technique	Nickel type	Enhanced property	Ref.
PMDA-ODA	UV irradiation	Electroless Ni	Electronic	[113]
PMDA/ODA	Microplasma	Ni films	Microcavity	[115]
PMDA/BPDA	Ion etching	$NiSO_4{\cdot}6H_2O$	Photocatalytic	[116]
PMDA/ODA	Hot press	NiCrBSi	Tribological	[117]
PMDA/ODA	Electron beam	Ni zone plates	Diffraction	[118]
ODA/PMDA	UV irradiation	$NiCl_2{\cdot}6H_2O$	Catalytic	[119]
PMDA/ODA	UV radiation	NiO	Thermal	[120]

precursors having enhanced properties such as spintronics, crack control, mechanical, and thermal properties.

In situ techniques gained popularity because they are easy to implement and result in the production of PI films with a homogeneous distribution of metal nanoparticles [126]. These techniques are suitable for conjugated polymers which is an added advantage. However, the conversion of precursors to metal nanoparticles within the PI matrix can result in the deposition of undesirable side reactions in the PI matrix [127]. The fabrication of PINiNCs by *in situ* single stage techniques are shown in Table 8.

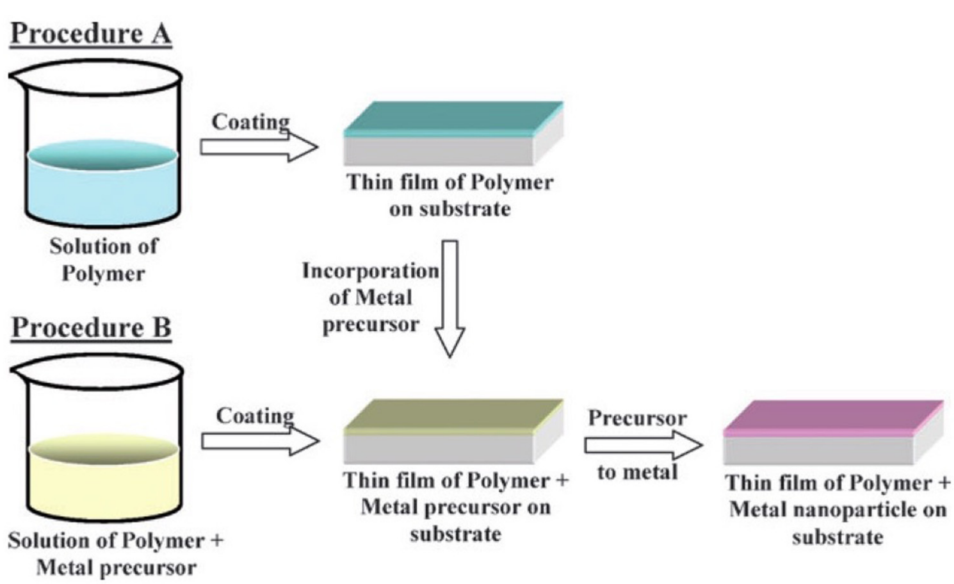

Figure 7: Typical *in situ* procedure for the fabrication of PI metal composite [125].

3.3 Surface modification

Metallized PI matrices are widely employed in flexible electronics due to their modified surface properties [133]. A variety of surface modification techniques for the fabrication of PI nickel composite films are reported in the literature [134]. Recently PI surface mechanism has received a lot of attention due to insulation failure of PI films under pulse voltage. Surface charge has great effect on dielectric properties, characteristics of direct current flashover, and rising time of pulse voltage [135]. Therefore, surface modification is required to enhance the surface properties of PIs by incorporation of conductive metal fillers.

Liu *et al.* [136] reported the successful surface modification of as-synthesized PI films prepared from PMDA and ODA monomers. The surface modification involved four stages including alkaline hydrolysis of the PI film by KOH, ion exchange by Ni, catalytic reduction of Ni nanoparticles, and finally, electroless deposition of Ni as shown in Figure 8. Surface modification techniques have several advantages, for instance, high temperature annealing is not required, no need for vacuum conditions, and no expensive experimental setup needed for the preparation of samples.

In their detailed procedure, the PI films were cut into pieces and cleaned using ultrasonic ethanol bath. Thereafter, the PI films were rinsed with deionized water dried in an oven. The PI films were then immersed in KOH solution. Imide ring cleavage in the PI occurred due to alkaline hydrolysis in KOH. Afterward, the PI films were rinsed with deionized water. The PI films were immersed in $NiCl_2$ solution to perform the ion exchange reaction. The Ni ions exchanged with the implanted K^+ ions of the treated PI film. Table 9 shows a surface modification technique for the synthesis of PI nickel composites.

Surface modification techniques have several advantages, for instance, high temperature annealing is not required, no need for vacuum conditions, and no expensive experimental setup needed for the preparation of samples [144]. However, certain shortcomings of surface modification techniques are apparent such as excessive ring cleavage reactions may occur during hydrolysis and acid–base neutralization reaction between carboxylic acid and K^+ ions can lead to the formation of a complex with PI [145].

3.4 Direct printing technique

Direct printing method is one of the promising techniques to fabricate thin films of Ni on PI substrate [146]. Printable metal current collectors are cost effective and can be operated at a wide range of operational voltage [147]. PI surface modification by the introduction of a nanoscale coupling agent enhances the attachment of metal atoms on the PI through wet deposition [148]. Whereas in the dry technique, the PI surface is modified by pretreatment of the plasma to generate reactive sites which strengthen the bonding between PI and metal atoms [149]. Figure 9 represents the stages in the direct printing technique of Ni on photoreactive PI. Figure 9 shows the procedure for fabricating solid-state micro-supercapacitors devices by printing sequentially the Ni current collector, graphene electrode, and ionic liquid-based gel-like electrolyte on the PI substrate.

Chae *et al.* [147] described the fabrication of direct printable metallic current using chemically synthesized NiNPs. The printable fluid comprises NiNPs, Ni flakes, and a polyvinyl pyrrolidone photoreactive binder mixture. The metallic current collector was generated by flashlight sintering reaction. The direct printed particulate layer was converted to metallic current collector with robust electrochemically conductive surface layer. The conductive fluid is then printed, followed by polymerization. Table 10 presents the direct printing of Ni on PI substrate using various techniques.

The direct printing technique allows both current and voltage to be controlled easily in a constructed power source. The major advantage of direct printing approach is the possibility of formulating multitasked devices without employing

Table 8: Summary of *in situ* fabrication techniques for PINiNCs

PI monomers	Fabrication technique	Nickel type	Enhanced property	Ref.
PMDA/ODA	Single stage	Ni–Fe	Spintronics	[128]
ODA/PMDA	Deposition	Ni thin film	Crack control	[129]
PMDA/ODA	Plating	Ni–W–P	Electromagnetic	[66]
PMDA/ODA	Imidization	$Ni(CH_3COO)\cdot 4H_2O$	Electrochemical	[130]
ODA/PMDA	Electrodeposition	$NiSO_4\cdot 6H_2O$	Electrocatalysis	[131]
6FDA-DDS	*In situ* generated	Ni nanoparticles	Structural	[125]
PMDA/ODA	Electrospinning	$Ni(NO_3)_2\cdot 6H_2O$	Electrochemical	[132]

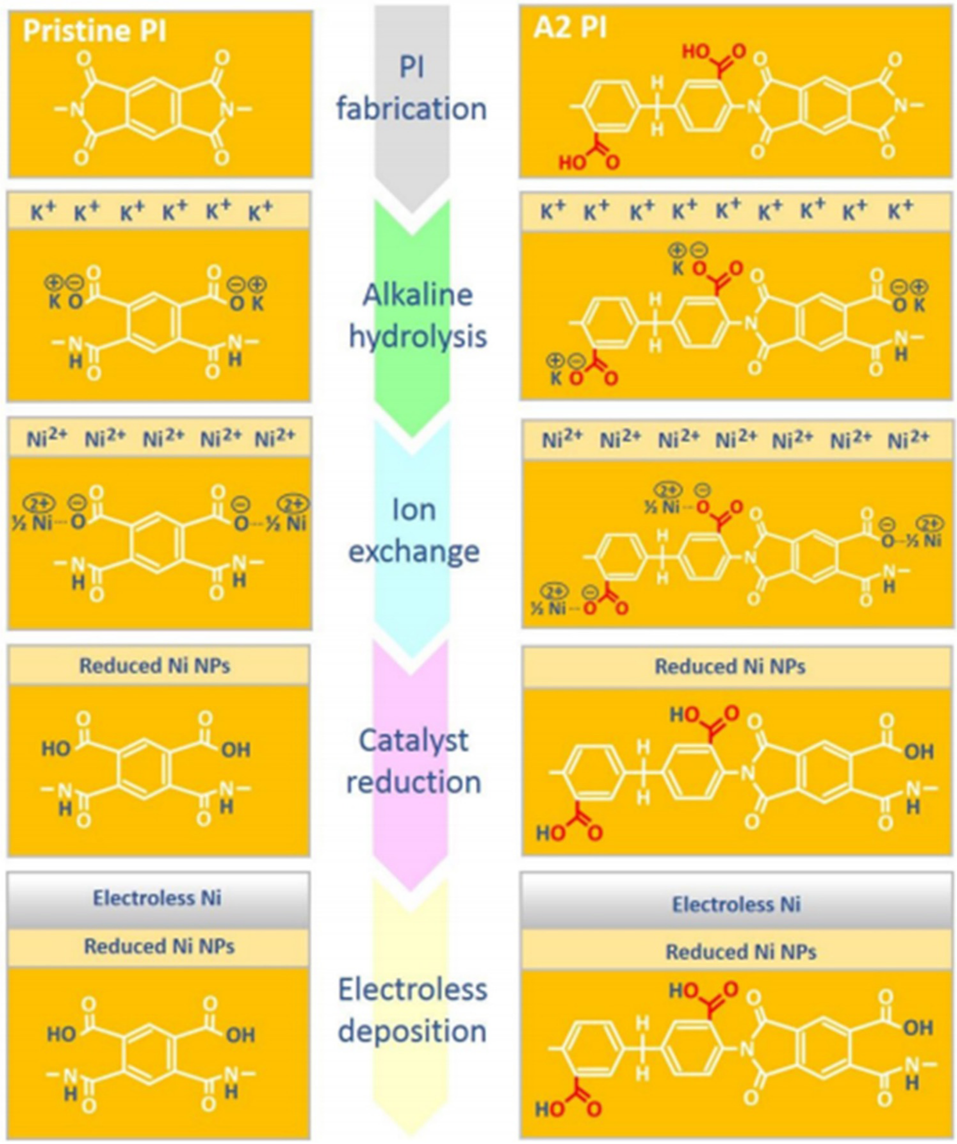

Figure 8: Surface modification flowchart of PI film and electroless deposition of Ni [136].

Table 9: Summary of surface modification techniques for the fabrication of nickel composites

PI monomers	Fabrication technique	Nickel type	Enhanced property	Ref.
PMDA/ODA	Ni plating	Ni–Cr alloy	Adhesion	[137]
ODA/PMDA	Sputtering	Ni nanoparticles	Electronic	[138]
PMDA/ODA	Deposition	$NiSO_4 \cdot 6H_2O$	Catalytic	[139]
ODA/PMDA	Roll-to-roll	$NiCl_2 \cdot 6H_2O$	Incorporation	[140]
PMDA/ODA	Electroplating	$NiCl_2 \cdot 6H_2O$	Adhesion	[141]
PMDA/ODA	Ink-jet printing	Ni–Cr	Electrochemical	[142]
PMDA/ODA	Sintering	Ni nanoparticles	Electrochemical	[143]

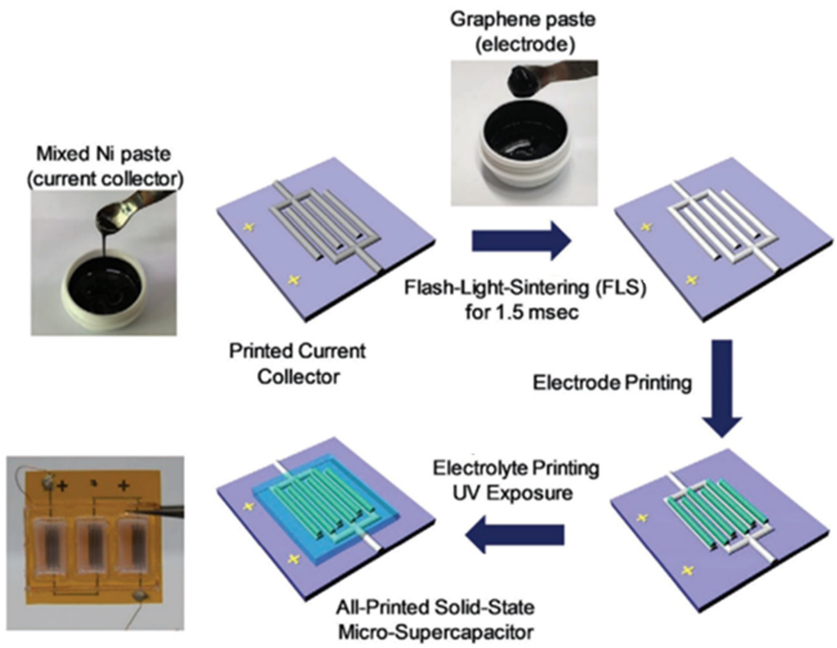

Figure 9: Direct printing of Ni on PI substrate [147].

Table 10: Summary of direct printing techniques for Ni on PI substrate

PI monomers	Fabrication technique	Nickel type	Enhanced property	Ref.
ODA/PMDA	Inkjet printing	NiO powder	Flexibility	[150]
PMDA/ODA	Inkjet printing	$NiCl_2{\cdot}6H_2O$	Capacitance	[146]
PMDA/ODA	Ni plating	NiO	Anti-scratch	[151]
PMDA/ODA	Laser annealing	Ni (111)	Conductivity	[152]
ODA/PMDA	Laser writing	Ni ions	Conductivity	[153]
PMDA/ODA	Sputtering	Ni–Ti	Crystallinity	[154]
PMDA/ODA	Incorporation	Ni nanoparticles	Adhesion	[140]

complicated procedures. Direct printing has the disadvantages of synthesis and printing techniques requiring moisture free and controlled atmosphere which are difficult conditions to attain in the laboratory.

3.5 Sputtering technique

Magnetron sputtering is the most widely employed technique to deposit atomic Ni complex films among the physical vapor deposition methods [155]. Thin films of Ni complex such as Ni–Ti can be deposited at ambient or high temperatures. Submicron films of Ni–Ti exhibit shape memory effect and are therefore promising components for silicon-based memory devices [156]. It requires metal to be sputtered on the PI substrate, ultra-sonicated with solvent to remove impurities, and photolithography between Ni and PI substrate to improve the adhesion. Figure 10 is a schematic representation of magnetron sputtering of Ni on thin film substrate. In the figure, the sputtering targets are 60^{o} inclined to each other in confocal geometry located on top of the chamber facing the substrate platform. Nickel films of thickness varying from 150 to 250 nm were deposited from 3 in nickel target onto 1″ × 1″ silicon substrate using direct current magnetron sputtering technique. The substrates were centrifuged at a speed of 26 rpm to maintain uniformity in the resulting thin films.

Wang *et al.* [157] reported the fabrication of flexible shear stress sensor composed of Ni thermistors and Cu electrodes. In their procedure, 0.3 μm thick Ni thermistor with both ends stacked to parallel Cu electrodes is sputtered on the PI substrate. The PI substrate is attached to the glass and ultrasonicated with acetone, ethanol, and distilled water to remove impurities. The PI is then placed in a drying machine to dry the substrate. The reverse is spun on the PI substrate at 3,000 rpm. The photolithography pattern is transferred to the photoresist. Finally,

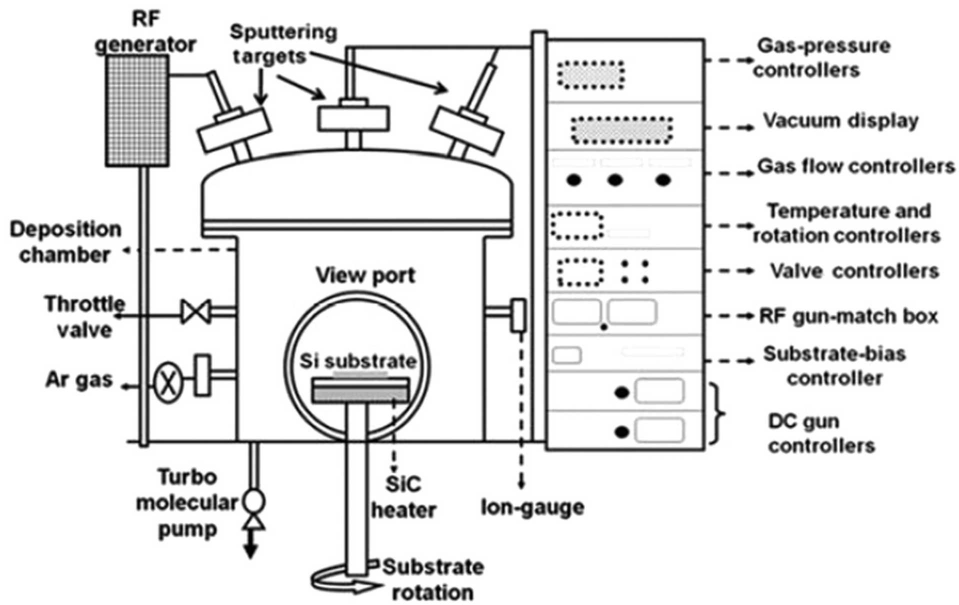

Figure 10: Schematic representation of magnetron sputtering of Ni on substrate [68].

NiNPs are sputtered on the substrate with photoresist pattern. Chromium film is then deposited between the Ni and PI substrate to improve the adhesion of Ni film on the PI substrate. The sputtering techniques of Ni on PI substrate are summarized in Table 11.

Sputtering technique has the advantage of depositing near-equiatomic and equiatomic Ni composites. Similarly, the technique enables the production of flexible shear stress devices that can be attached to any surfaces irrespective of their shapes. However, annealing treatment on the performance of these devices has not been fully studied. Furthermore, the appropriate annealing temperature and time need to be determined to meet the required adhesion strength, resistance, and temperature coefficient of resistance [157].

3.6 Conventional mixing/sol–gel technique

Conventional mixing or sol–gel technique is widely employed in the preparation of PINiNCs. This technique provides the prospect of fabricating distinct nanocomposite materials with fine-tuned and novel properties by adopting versatile and simple methods. Sol–gel technique is regularly used in the preparation of glass materials and ceramics at ambient temperatures [163]. The technique is an outstanding method for the fabrication of bioglasses in which the system undergoes a transition from colloidal mixture (sol) into solid (gel) and has been employed for large-scale production at low cost [164]. Moreover, the techniques represent a method with low environmental impact and low cost of production such as roll-to-roll, blade and spray coating on metal foils, flexible polymeric

Table 11: Summary of sputtering techniques for the fabrication of PINiNCs

PI monomers	Fabrication technique	Nickel type	Enhanced property	Ref.
PMDA/ODA	Co-sputter	Ni-rich Ni–Ti	Electrochemical	[155]
PMDA/ODA	Sputtering	Ni nanoparticles	Mechanical	[158]
PMDA/ODA	Sputter	Ti–Ni–Cu films	Mechanical	[159]
ODA/PMDA	Sputtering	Ni thermistor	Thermal	[109]
PMDA/ODA	Sputtering	Ni–Ti thin films	Mechanical	[160]
PMDA/ODA	Sputtering	Ni micro	Capacitance	[161]
PMDA/ODA	Sputtering	Ni–Ti	Mechanical	[162]

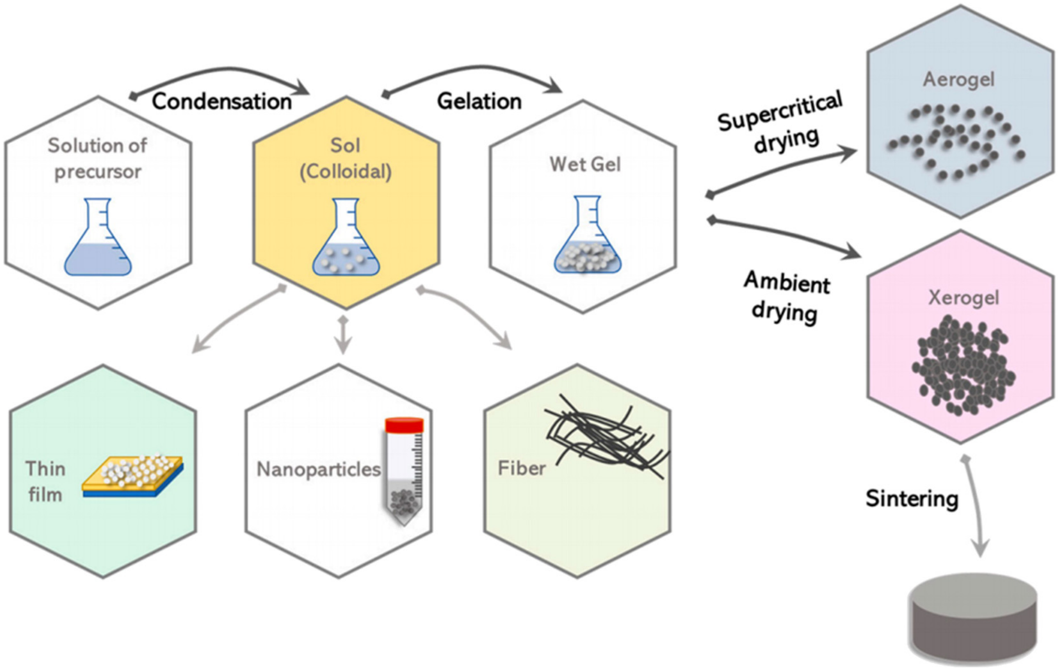

Figure 11: Schematic representation of products processed using sol–gel techniques [163].

Table 12: Summary of sol–gel techniques for the fabrication of PINiNCs

PI monomers	Fabrication technique	Nickel type	Enhanced property	Ref.
PMDA/ODA	Spalling	Ni	Piezoelectric	[167]
PMDA/ODA	Sol–gel	NiO	Optical	[168]
ODA/PMDA	Sol–gel	$NiMn_2O_4$	Sensing	[166]
PMDA/ODA	Aerogel	$Ni(NO_3)_2{\cdot}6H_2O$	Electrochemical	[169]
ODA/PMDA	Imidization	Ni powder	Ionic conductivity	[170]
BAPP/BPDA	Spin coating	Ni complex	Interlocking effect	[171]
PMDA/ODA	Implantation	Ni–Cr	Toughness	[172]

substances, and inkjet printing [165]. Figure 11 shows a representation of various products by sol–gel techniques. The formation of a sol, a stable suspension of colloidal particles in a liquid occurs in the initial stage *via* fast hydrolysis reaction. The alkoxide moiety in the reaction is changed by the hydroxyl group. Furthermore, condensation takes place before hydrolysis comes to an end. The drying stage involves the removal of the liquid phase and a xerogel can be obtained.

Dojcinovic *et al.* [166] prepared PINiNCs by using sol–gel technique. In their report, sodium alginate gel was prepared by mixing alginic sodium salt in deionized water using magnetic stirrer for 6 h at ambient temperature, followed by adding the cross-linking agent calcium chloride and glycerol with continuous gentle mixing. In the next step, prepared nickel magnetite powder was added to the gel and mixed through ultrasonic dispersion. Finally, the nanocomposite gel was casted drop-wise onto Kapton PI substrate and allowed to dry at ambient temperature for few days to form a thin film of PINiNC. Table 12 shows a summary of various PINiNCs prepared using sol–gel techniques.

The principal advantages of sol–gel technique are the incorporation of thermolabile fillers into the polymer matrix and the purity of the obtained products [173]. Similarly, the sol–gel techniques have allowed for large-scale production at low cost in addition to the versatility of the fabricated products ranging from inorganic, organic, metallic, and hybrid nanocomposites. However, the sol–gel techniques requirement for fabrication temperature monitoring may constitute a drawback of the techniques.

4 Properties of PINiNCs

4.1 Chemical structure of PINiNCs

The chemical structure determination of PINiNCs is carried out to investigate the relationship between structure and properties of the nanocomposites. The most widely employed characterization techniques in chemical structure determination are Fourier transform infrared spectroscopy (FT-IR), nuclear magnetic resonance, gel permeation chromatography, energy dispersive X-ray, and elemental analysis. FT-IR is widely used to confirm the formation of PI. The FT-IR spectra of PI firms prepared by thermal imidization show the characteristic absorption bands of PI at about 1,780 cm^{-1} (C═O of cyclic imide asymmetric stretching vibration), 1,720 cm^{-1} (C═O of imide symmetrical stretching vibration), and 1,380 cm^{-1} (C–N imide stretching vibration) [41,82,136,174]. The characteristic imide absorption bands are shown in Figure 12.

The characteristic absorption band for most inorganic materials, including NiNPs corresponds to the long wavelength transverse optical mode and the optical photon frequency that occur between 390 and 403 cm^{-1} [176]. The Ni–O phase formation is a broad absorption band in the region of 820–400 cm^{-1} assigned to Ni–O stretching vibration mode [177]. In the IR spectra, the interaction between PI and NiO occurs because of the partial hydrolyzation on the outer surface of NiO leading to the formation of OH groups. The O–H stretching vibrations appear at about 3,427 cm^{-1} [41]. The PI and NiO are held together by hydrogen bonding provided by the hydroxyl groups, these groups are as shown in Figure 13.

4.2 Morphological properties of PINiNCs

The morphology of PINiNCs depends on factors such as configuration and conformation of their macromolecules, chemical composition of monomers units, the presence of various additives, and inorganic NiNPs. The structure of the polymeric material undergoes changes during its processing including different degrees of the polymer composites [56] crystallinity as well as melting point interval [178]. Hence there is a need for morphological characterization to investigate the metallization uniformity and to determine the interior microstructure of PINiNCs. The widely used characterization techniques for PI composites morphology and topology are field emission scanning electron microscopy, transmission electron microscopy (TEM), X-ray photoelectron spectroscopy (XPS) [179], and atomic force microscopy (AFM) [180]. Figure 14 shows typical cross-sectional TEM images of (a) PI containing NiNPs and (b) enlarged image of the NiNPs in PI matrix.

The PI and NiNPs interfacial layer showed granular appearance due to the presence of catalytic NiNPs resulting from their reduction during the metallization process. The images show that the granular NiNPs did not aggregate in confined regions of the PI indicating that the base treatment leading to ion exchange of K^+ ions from KOH and Ni ions played a significant role in the generation and subsequent distribution of reduced NiNPs.

4.3 Physical properties of PINiNCs

The physical properties of PI composites are investigated by several techniques including X-ray diffraction (X-RD),

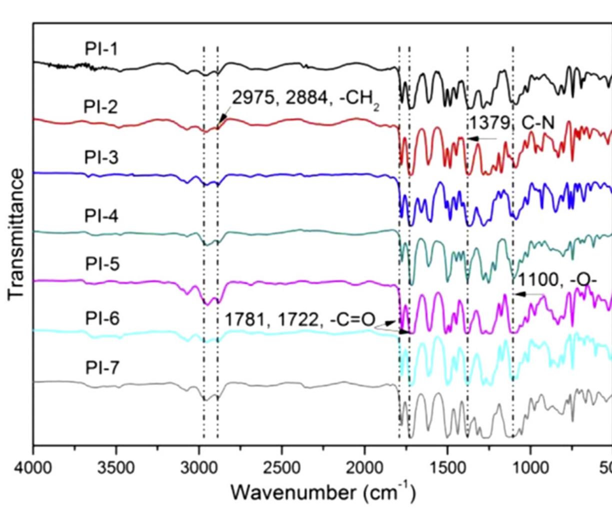

Figure 12: Characteristic FT-IR absorption spectra of PIs [175].

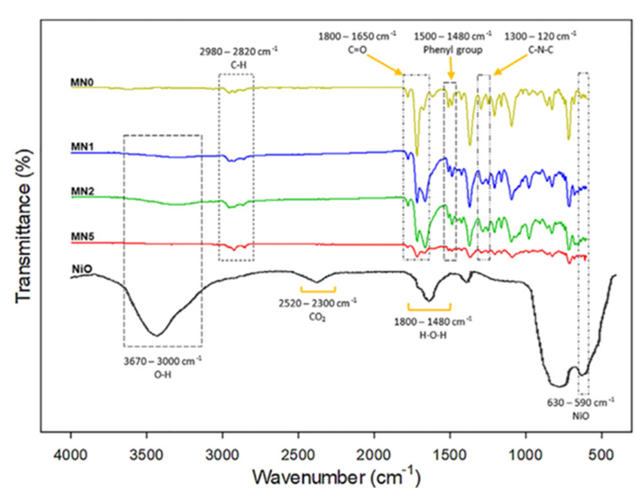

Figure 13: IR spectra of PI and NiO interaction [41].

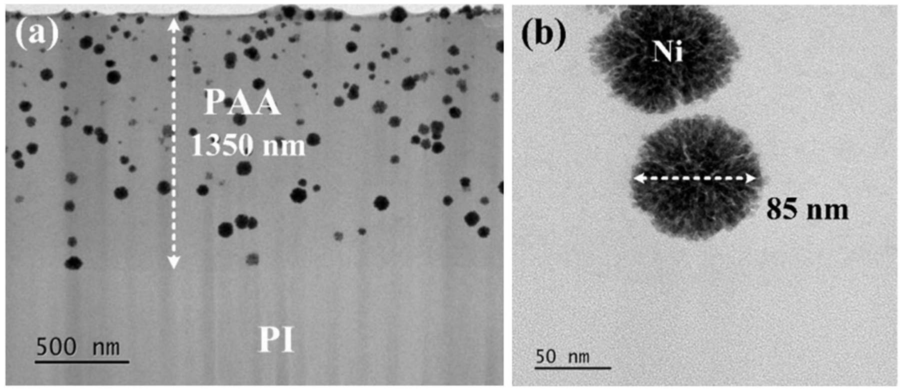

Figure 14: Cross-sectional TEM images of (a) PI film containing NiNPs and (b) enlarged image of NiNPs [42].

ultraviolet–visible spectroscopy, XPS, AFM, and several other techniques [181]. X-RD is the standard technique for crystallographic structure determination. The technique enables the determination of crystal size and perfection, the crystallinity, the degree of orientation in the PI composites as well as the conformation of chains in amorphous PIs. Similarly X-RD is used to accurately determine lattice spacing in a crystalline PI nanocomposite [182]. Figure 15 shows the X-RD patterns of PI loaded with Ni^{2+} after urea treatment and thermal imidization.

In the figure Gao *et al.* [105] reported diffraction patterns corresponding to phase pure carbon and pure metallic Ni phase. Moreover, the observed slight peak shift to low angle in comparison to pure Ni phase indicates an expansion of the lattice due to carbon occupation from the PI matrix and carbon nanotubes.

4.4 Mechanical properties of PINiNCs

The surface and near-surface mechanical properties of PI composite thin films and coatings are crucial to their applications and final performance. The mechanical properties of PINiNCs and their correlations are essential prerequisite in understanding their design and applications [183]. Recently, mechanical properties of thin films are evaluated by depth-sensing nanoindentation techniques to investigate their tensile strength, tensile modulus, and elongation at break [184]. Mohri *et al.* [185] reported the mechanical properties of PI–Ni-rich composites. The Ni-rich PI–NiTi nanocomposite deformation occurred in four stages: elastic deformation austanite of the parent phase, martensitic transformation due to tress, martensitic phase elastic deformation, and martensitic plastic deformation. Similarly, Zhang *et al.* [186] investigated the effect of particle size distribution on the mechanical properties of bio-composites. They concluded that the embedded particles provided more cross-linking points in the polymer matrix. The force–strain curves of PI–Ni-rich and PI composites are shown in Figure 16. The nanocomposite and PI are both under isostrain and the measured force is the sum of the forces on both layers.

The force–stress curve shows that the PINiNC film possesses enhanced strength and ductility for all practical purposes. The remarkable enhancement in mechanical properties is attributed to the nanostructure of the composite. In the PI the nucleated surface cracks grow unstably due to homogeneous material rigidity. However, in the Ni-rich nanocomposite the growth of nucleated crack is impeded by the presence of the NiNPs [185].

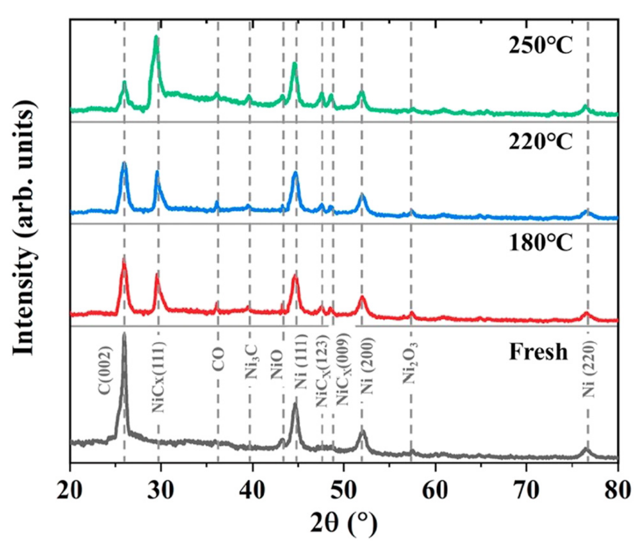

Figure 15: XRD patterns of PI loaded with NiNPs and annealing temperatures [105].

4.5 Electrical properties of PINiNCs

The most widely employed electrochemical techniques for the characterization of PINiNCs are conductometry, amperometry, potentiometry and voltammetry. The sample is investigated by measuring the potential in volts and current in amperes in an electrochemical cell containing the analyte. Electrochemical techniques are based on the measurement of the response of an electrochemical cell containing an ion-conducting phase referred to as the electrolyte. Upon the application of electric input through electron-conducting electrodes immersed in the electrolyte the responses are recorded and used to characterize the sample. Electrochemical measurements represent advantageous techniques of characterization because electrode properties are analyzed *in situ* under relevant working conditions [187].

Okafor and Iroh [67] investigated the electrochemical properties of three electrodes, PI/Ni, PI/grapheme, and PI/porous graphene composite electrodes. The PI/Ni nanocomposite yielded results with remarkably higher specific capacitance and lower bulk resistance compared to both PI/graphene and PI/porous graphene electrodes as presented in Figure 17.

In the PINiNC the improved charge transfers and enhanced ionic diffusion processes across the material is promoted by the enhanced electrode/electrolyte interfacial contact due the presence of NiNPs.

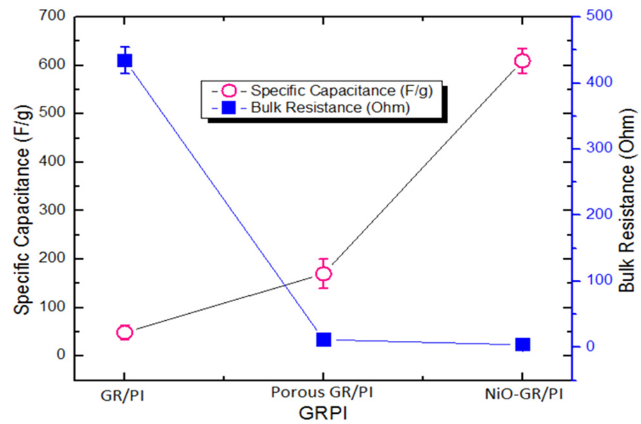

Figure 17: Comparison of electrochemical performance of PI/graphene, PI/porous graphene, and PI/Ni–graphene composites [67].

4.6 Magnetic properties of PINiNCs

The magnetic properties of materials are classified into five main categories including, intensity of magnetization, magnetic field, magnetic susceptibility, magnetic retentivity, and magnetic coercivity. The determination of these properties in PINiNCs is critical to produce high performance electromagnetic shielding nanomaterials with excellent absorption efficiency, predominantly suitable for microelectronic and aerospace flexible electronic applications [188]. Vibrating sample magnetometry is employed to investigate the magnetic properties of PINiNCs [189]. Wang and coworkers [30] fabricated multilayer-structured PI containing NiNPs. The magnetization of the samples increased significantly on increasing the NiNP content from 20 to 50%. The increase in NiNPs resulted in magnetization of 16.7–33.2 emu·g^{-1}. Figure 18 shows the magnetic hysteresis loops at various Ni content.

The addition of NiNPs enhanced the magnetic properties of the PI; the prominent magnetic properties predispose the nanocomposite as promising candidate for

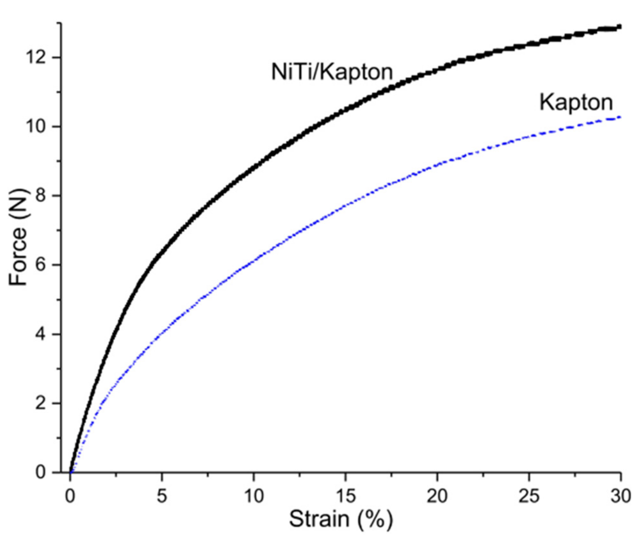

Figure 16: Force–strain curves of PINiNC and bear PI [185].

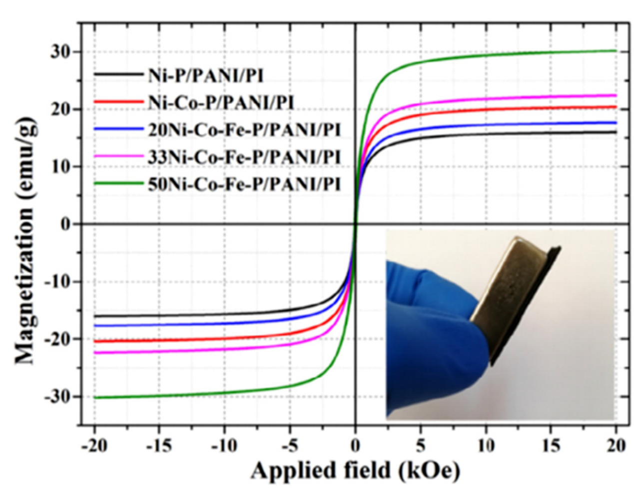

Figure 18: Magnetic hysteresis loops at various Ni content [30].

electromagnetic shielding material with excellent absorption properties.

5 Applications of PINiNCs

5.1 Lithography applications of PINiNCs

Recently, the demand for miniaturized and highly compact devices has attracted attention in technological research. The advantages of these technologies like lithography are the adaptability to various surface configurations where PI substrate is patterned with NiNPs to develop electronic devices with applications in biomedical fields and industrial applications. The lithography applications of PINiNCs are presented in Table 13.

5.2 Biomedical applications of PINiNCs

In the last decade researchers have developed prototype sensors using PINiNCs which offer beneficial medical applications. In general, polymer-based nanocomposites are employed as carrier or constructional material in the human body [196]. In the medical fields various intrinsic and extrinsic chronic and acute infectious diseases are monitored with flexible sensors. NiNPs in the range of a few nanoparticles to microns are used to form the sensing points of the prototype sensors. The developed sensors are employed in numerous medical applications such as body movements, monitoring of physiological parameters, and chemical changes occurring in the body systems. Table 14 shows various medical applications of PINiNCs.

5.3 Application of PINiNCs as electrodes

PI is among the polymeric precursor material for the fabrication of electrodes due to its inertness to chemical attack, superior thermal stability, excellent mechanical properties, and radiation shielding effects [204]. PIs containing Ni are promising electrode materials due to their fast redox properties, cost effectiveness, and low environmental toxicity. The application of PINiNCs as electrodes is presented in Table 15.

Table 13: Applications of PINiNCs in lithography

PI monomer	Ni type	Lithography applications	Ref.
PMDA/ODA	NiNPs	Diode	[190]
PMDA/ODA	Ni silicide	Transistors	[191]
ODA/PMDA	Ni film	Microwave	[192]
PMDA/ODA	NiNPs	Micro-heater	[193]
ODA/PMDA	Ni layer	Micro-batteries	[194]
ODA/PMDA	NiNPs	Textile metallization	[195]
ODA/PMDA	Ni–Cr	Elastic photomask	[172]

Table 14: Medical applications of PINiNCs

PI monomer	Ni type	Biomedical applications	Ref.
ODA/PMDA	Ni	Sensor	[197]
PMDA-ODA	$NiCl_2$	Cell sorting	[198]
PMDA/ODA	Ni powder	Radiation shielding	[199]
BTDA/ODA	Ni scaffold	Acquisition of bio-signals	[200]
PMDA/ODA	Cu/Ni layer	Humidity sensor	[201]
BTDA/ODA	$Ni(NO_3)_2{\cdot}6H_2O$	Interference shielding	[202]
PMDA/ODA	Ni complex	Microwave absorption	[203]

5.4 Applications of PINiNCs as membrane

PI materials are extensively used in gas separation membranes due to their high gas selectivity. Membrane technology to a large extent is dependent on high performance membrane materials such as PIs containing inorganic materials. Incorporating Ni complex framework nanocrystals into PI matrix improves their anti-plasticization properties [211]. Similarly, monolithic piezoelectric materials exhibit a range of notable directionality and coupled properties. However, the use of composite materials such as PINiNCs significantly improves these shortcomings [212]. Therefore, PINiNCs exhibit unique properties necessary in the fabrication of gas separation membranes. Selected PINiNCs reported in literature are presented in Table 16.

5.5 Dielectric application of PINiNCs

PI composites with low dielectric constant are widely employed as interlayer and packaging materials in

Table 15: Application of PINiNCs as electrode materials

PI substrate	Ni constituent	Electrode applications	Ref.
PMDA/ODA	Ni layer	Ni-rich cathode	[205]
BPDA/ODA/PDA	Nickel nitrate	Photocatalytic	[27]
ODA/PMDA	Ni foil	Lithium-ion batteries	[206]
PMDA/ODA	Ni layer	Wire-type electrode	[207]
ODA/PMDA	$Ni(OH)_2$	Electrochemical probe	[208]
PMDA/ODA	$NiCl_2{\cdot}6H_2O$	Working electrodes	[209]
PMDA/ODA	$Ni/Zn/Fe_2O_4$	Microwave circuit	[210]

Table 16: Selected PINiNCs in membrane applications

PI monomer	Ni type	Membrane application	Ref.
6FDA/DAM	Ni gallate	Gas separation	[213]
6FDA-Durene	Ni nanoparticles	Gas separation	[214]
BPDA/DAB/MMB	Ni-foam	Supercapacitors	[211]
BTDA/ODA	$NiCo_2O_4$ nanowire	Microelectronic systems	[202]
PMDA/ODA	$NiCl_2$	Wearable electronics	[215]
6FDA/BTDA	Ni complex nanocrystals	Plasticization resistance	[216]
BTDA/ODA	$Ni(NO_3)_2{\cdot}6H_2O$	Electromagnetic shielding	[217]

microelectronic industry due to their excellent thermal stability, unique physicochemical properties, as well as good chemical and radiation resistance [218]. PINiNCs employed as interlayer materials in high density integrated circuits, can significantly reduce power dissipation, time delay, and cross-talk time. PI dielectrics play a key role in the fabrication of flexible, scalable devices, and integrated circuits for organic electronic devices [219]. The applications of PINiNCs in dielectrics are presented in Table 17.

5.6 Applications of PINiNCs in light emitting diode (LED) devices

Modern optoelectronic devices consist of transparent electrodes such as in LEDs, touch-screen displays, and solar cells. Indium tin oxide is a major component of LEDs. However, the high cost of indium leads to expensive products. Recently, research groups have focused on alternative transparent electrodes that are ultrathin, flexible, and light weight [223]. Metal grids with excellent conductivity, mechanical flexibility, and transparency are promising candidates for the replacement of indium tin oxide in LEDs. Transparent colorless PI films prepared using BPADA precursor can replace the glass in liquid crystal display devices [224]. Recently, metal grids have been prepared by facile technique in the production of LEDs [225]. The metal grids are deposited on a transparent PI film. Metallic films embedded into PI matrix generate a periodically inhomogeneous thermal field. The homogeneous thermal field is henceforth transformed into functionally gradient phononic crystals [226]. LEDs with transparent PI substrate containing Ni are presented in Table 18.

Table 17: Dielectric applications of PINiNCs

PI monomer	Preparation technique	Ni type	Dielectric application	Ref.
ODA/PMDA	Co-precipitation	$Ni(NO_3)_2{\cdot}6H_2O$	Microwave absorption	[101]
PMDA/ODA	Solution blending	Ni nanowires	Aerospace application	[220]
PMDA/PPD	Liquid–solid–solid	$Ni(acac)_2$	Microwave absorption	[89]
ODA/PMDA	Electrodeposition	$NiSO_4{\cdot}H_2O$	Shielding material	[188]
PMDA/ODA	Mechanochemical	NiO–Mg	Discharge devices	[221]
PMDA/ODA	Electrodeposition	Ni oxide	Capacitor	[67]
ODA/PMDA	*In situ* bending	Ni metal	Flexible dielectrics	[222]

Table 18: PIs containing Ni and their applications in LEDs

PI monomer	Preparation technique	Ni type	Dielectric application	Ref.
ODA/PMDA	Electrodeposition	Ni/Au layers	Deformable LED	[227]
PMDA/ODA	Vapor deposition	Ni film	Pressure sensors	[228]
PMDA/ODA	Screen printing	Ni ink	Flexible microdevice	[229]
PMDA/ODA	Electrodeposition	Ni/Au layer	Multicolor LED	[230]
ODA/PMDA	Pattern transfer	Ni–Cu alloy	Wearable electronics	[231]
PMDA/ODA	Lamination	Ni foil	Thermoelectric devices	[232]
PMDA/ODA	e-beam evaporation	Ni nano	Optoelectronic devices	[233]

6 Conclusion

In this review, we focused on the strategies to fabricate novel PINiNCs. Various modern cutting-edge characterization technologies for PINiNCs have been emphasized. The industrial applications of PINiNCs have been thoroughly reviewed to develop a complete reference material on PINiNCs. We herein critically report the design and fabrication methodologies of PINiNCs. The recent characterization probing techniques and applications, revealing their advantages and disadvantages are examined in depth. Their diverse applications in multidisciplinary as well as high technological fields and their corresponding properties are extensively documented and summarized in tables. This article should provide inspiration for the preparation, characterization, and applications of PINiNC materials; moreover, to pave the way for the critical assessment of their engineering and industrial applications. As a result, future work on PINiNCs will focus on new multifunctional PINiNCs and advanced materials including the synthesis of new hybrids and new types of PI nanocomposites. Current trends and opportunities for the fabrication of PINiNCs include 3D membrane printing, fused filament fabrication for 4D printing, and aqua-membrane spacer printing technology.

Acknowledgments: The authors would like to thank the School of Chemical Sciences, Universiti Sains Malaysia for technical support.

Funding information: The authors wish to acknowledge Universiti Sains Malaysia for FRGS/1/2020/STG05/USM/02/3 awarded by the Ministry of Higher Education Malaysia. Nuru-Deen Jaji wishes to thank the Federal College of Education Technical Gombe, Nigeria, for TETFUND Postgraduate Scholarship.

Author contributions: Muhammad Bisyrul Hafi Othman and Hazizan Md Akil: conceptualization and resources. Nuru-Deen Jaji: formal analysis and investigation. Muhammad Bisyrul Hafi Othman and Hooi Ling Lee: Nuru-Deen Jaji: data curation, writing, and original draft preparation. Muhammad Bisyrul Hafi Othman, Hooi Ling Lee, Mohd Hazwan Hussin, Zulkifli Merican Aljunid Merican, and Mohd Firdaus Omar. Muhammad Bisyrul Hafi Othman: project administration. All authors have accepted responsibility for the entire content of this manuscript and approved its submission.

Conflict of interest: The authors state no conflict of interest.

References

[1] Bledzki, A. K., H. Seidlitz, K. Goracy, M. Urbaniak, and J. J. Rösch. Recycling of carbon fiber reinforced composite polymers—review—Part 1: volume of production, recycling technologies, legislative aspects. *Polymers*, Vol. 13, No. 2, 2021, pp. 300–313.

[2] Giannelis, E. P. Polymer-layered silicate nanocomposites: synthesis, properties and applications. *Applied Organometallic Chemistry*, Vol. 12, No. 10–11, 1998, pp. 675–680.

[3] Gandhi, R. A., K. Palanikumar, B. Ragunath, and J. P. Davim. Role of carbon nanotubes (CNTs) in improving wear properties of polypropylene (PP) in dry sliding condition. *Material and Design*, Vol. 48, No. 1, 2013, pp. 52–57.

[4] Padua, L. M. G., J. M. Yeh, and K. S. Santiago. A novel application of electroactive polyimide doped with gold nanoparticles: as a chemiresistor sensor for hydrogen sulfide gas. *Polymers*, Vol. 11, No. 12, 2019, pp. 1918–1934.

[5] Kumar, V., A. Kumar, M. Song, D. J. Lee, S. S. Han, and S. S. Park. Properties of silicone rubber-based composites reinforced with few-layer graphene and iron oxide or titanium dioxide. *Polymers*, Vol. 12, No. 10, 2021, pp. 1550–1567.

[6] Yuan, Y., Y. T. Pan, Z. Zhang, W. Zhang, X. Li, and R. Yang. Nickle nanocrystals decorated on graphitic nanotubes with broad channels for fire hazard reduction of epoxy resin. *Journal of Hazardous Materials*, Vol. 402, No. 1, 2021, pp. 123880–123889.

[7] Martin, R. C., E. Locatelli, Y. Li, P. Matteini, I. Monaco, G. Cui, et al. One-pot synthesis of magnesium nanoparticles embedded in a chitosan microparticle matrix: a highly biocompatible tool for in vivo cancer treatment. *Journal of Materials Chemistry B: Materials for Biology and Medicine*, Vol. 4, No. 2, 2016, pp. 207–211.

[8] Han, E., D. Wu, S. Qi, G. Tian, H. Niu, G. Shang, et al. Incorporation of silver nanoparticles into the bulk of the electrospun ultrafine polyimide nanofibers *via* a direct ion exchange self-metallization process. *ACS Applied Materials & Interfaces*, Vol. 4, No. 5, 2012, pp. 2583–2590.

[9] Son, S. R., J. An, J. W. Choi, and J. H. Lee. Fabrication of TiO_2-embedded polyimide layer with high transmittance and improved reliability for liquid crystal displays. *Polymers*, Vol. 13, No. 3, 2021, pp. 376–388.

[10] Yan, P., Y. Shen, X. Du, and J. Chong. Microwave absorption properties of magnetite particles extracted from nickel slag. *Materials*, Vol. 13, No. 9, 2020, pp. 2162–2177.

[11] Mamuru, S. A. and N. Jaji. Voltammetric and impedimetric behaviour of phytosynthesized nickel nanoparticles. *Journal of Nanostructure in Chemistry*, Vol. 5, No. 4, 2015, pp. 347–356.

[12] Jaji, N.-D., M. B. H. Othman, H. L. Lee, M. H. Hussin, and D. Hui. One-pot solvothermal synthesis and characterization of highly stable nickel nanoparticles. *Nanotechnology Reviews*, Vol. 10, No. 1, 2021, pp. 18–329.

[13] Jaji, N.-D., H. L. Lee, M. H. Hussin, H. M. Akil, M. R. Zakaria, and M. B. H. Othman. Advanced nickel nanoparticles technology: from synthesis to applications. *Nanotechnology Reviews*, Vol. 9, No. 1, 2020, pp. 1456–1480.

[14] Cheng, Y., M. Guo, M. Zhai, Y. Yu, and J. Hu. Nickel nanoparticles anchored onto Ni foam for supercapacitors with high specific capacitance. *Journal of Nanoscience and Nanotechnology*, Vol. 20, No. 4, 2020, pp. 2402–2407.

[15] Bhunia, K., S. Khilari, and D. Pradhan. Trimetallic PtAuNi alloy nanoparticles as an efficient electrocatalyst for the methanol

electrooxidation reaction. *Dalton Transactions*, Vol. 46, No. 44, 2017, pp. 15558–15566.

[16] Zingwe, N., E. Meyer, and J. Mbese. Synthesis, characterization and optimization of hydrothermally fabricated binary palladium alloys PdNix for use as counter electrode catalysts in dye sensitized solar cells. *Materials*, Vol. 12, No. 19, 2019, pp. 3116–3127.

[17] Handa, S., E. D. Slack, and B. H. Lipshutz. Nanonickel-catalyzed Suzuki–Miyaura cross-couplings in water. *Angewandte Chemie International Edition*, Vol. 54, No. 41, 2015, pp. 11994–11998.

[18] Li, N., Y. Li, Q. Li, Y. Zhao, C. S. Liu, and H. Pang. NiO nanoparticles decorated hexagonal nickel-based metal-organic framework: self-template synthesis and its application in electrochemical energy storage. *Journal of Colloid and Interface Science*, Vol. 581, No. Pt B, 2020, pp. 709–718.

[19] Castillo, C., K. Seguin, P. Aguirre, D. Venegas-Yazigi, A. D. C. Viegas, E. Spodine, et al. Nickel nanocomposites: magnetic and catalytic properties. *RSC Advances*, Vol. 5, No. 77, 2015, pp. 63073–63079.

[20] Wu, Q., W.-s Miao, H.-j Gao, and D. Hui. Mechanical properties of nanomaterials: a review. *Nanotechnology Reviews*, Vol. 9, No. 1, 2020, pp. 259–273.

[21] Pascariu, P., D. Vernardou, M. P. Suchea, A. Airinei, L. Ursu, S. Bucur, et al. Tuning electrical properties of polythiophene/nickel nanocomposites *via* fabrication. *Material and Design*, Vol. 182, No. 1, 2019, pp. 108027–108036.

[22] Kumar, G., N. K., Mogha, M., Kumar, Subodh, D. T., and Masram. NiO nanocomposites/rGO as a heterogeneous catalyst for imidazole scaffolds with applications in inhibiting the DNA binding activity. *Dalton Transactions*, Vol. 49, No. 6, 2020, pp. 1963–1974.

[23] Wang, Y., X. Yang, C. Hou, M. Zhao, Z. Li, Q. Meng, et al. Fabrication of $MnO_x/Ni(OH)_2$ electro-deposited sulfonated polyimides/graphene nano-sheets membrane and used for electrochemical sensing of glucose. *Journal of Electroanalytical Chemistry*, Vol. 837, No. 1, 2019, pp. 95–102.

[24] Flaifel, M. H. An approach towards optimization appraisal of thermal conductivity of magnetic thermoplastic elastomeric nanocomposites using response surface methodology. *Polymers*, Vol. 12, No. 9, 2020, pp. 2030–2046.

[25] Almeida, A. R., M. Salimian, M. Ferro, P. A. Marques, G. Goncalves, E. Titus, et al. Biochemical and behavioral responses of zebrafish embryos to magnetic graphene/nickel nanocomposites. *Ecotoxicology and Environmental Safety*, Vol. 186, No. 1, 2019, pp. 109760–109768.

[26] Zhang, X., X. Ni, C. Li, B. You, and G. Sun. Co-gel strategy for preparing hierarchically porous silica/polyimide nanocomposite aerogel with thermal insulation and flame retardancy. *Journal of Materials Chemistry A: Materials for Energy and Sustainability*, Vol. 8, No. 19, 2020, pp. 9701–9712.

[27] Lei, Y., J. Huo, and H. Liao. Microstructure and photocatalytic properties of polyimide/heterostructured $NiO–Fe_2O_3–ZnO$ nanocomposite films *via* an ion-exchange technique. *RSC Advances*, Vol. 7, No. 64, 2017, pp. 40621–40631.

[28] Mukherjee, S., S. Das, S. Nuthi, and C. R. Patra. Biocompatible nickel-prussian blue@silver nanocomposites show potent antibacterial activities. *Future Science OA*, Vol. 3, No. 4, 2017, pp. 233–251.

[29] Hamciuc, C., M. Asandulesa, E. Hamciuc, T. Roman, M. A. Olariu, and A. Pui. Novel polyimide/copper–nickel ferrite composites with tunable magnetic and dielectric properties. *Polymers*, Vol. 13, No. 10, 2021, pp. 1646–1661.

[30] Wang, Y., W. Wang, X. Ding, and D. Yu. Multilayer-structured Ni–Co–Fe–P/polyaniline/polyimide composite fabric for robust electromagnetic shielding with low reflection characteristic. *Chemical Engineering of Journal*, Vol. 380, No. 1, 2020, pp. 122553–122564.

[31] Slosarczyk, A., L. Klapiszewski, T. Buchwald, P. Krawczyk, L. Kolanowski, and G. Lota. Carbon fiber and nickel coated carbon fiber–silica aerogel nanocomposite as low-frequency microwave absorbing materials. *Materials*, Vol. 13, No. 2, 2020, pp. 400–418.

[32] Serbezeanu, D., T. Vlad-Bubulac, D. Rusu, G. Grădișteanu Pircalabioru, I. Samoilă, S. Dinescu, et al. Functional polyimide-based electrospun fibers for biomedical application. *Materials*, Vol. 12, No. 19, 2019, pp. 3201–3206.

[33] Abd, M. M., S. A. Salih, S. M. Baseem, A. N. Jasim, and M. A. Omar. Tensile properties of nickel epoxy nanocomposites prepared by combination ultrasonication and shear mixing methods. *Materials Today: Proceedings*, Vol. 20, 2020, pp. 448–451.

[34] Boychuk, V., V. Kotsyubunsky, K. V. Bandura, B. Rachii, I. Yaremiy, and S. Fedorchenko. Structural and electrical properties of nickel–iron spinel/reduced graphene oxide nanocomposites. *Molecular Crystals and Liquid Crystals*, Vol. 673, No. 1, 2019, pp. 137–148.

[35] Gopiraman, M., S. Saravanamoorthy, D. Deng, A. Ilangovan, I. S. Kim, and I. M. Chung. Facile mechanochemical synthesis of nickel/graphene oxide nanocomposites with unique and tunable morphology: applications in heterogeneous catalysis and supercapacitors. *Catalysts*, Vol. 9, No. 5, 2019, pp. 486–505.

[36] Li, J. Y., Z. M. Cao, Y. Hua, G. Wei, X. Z. Yu, W. B. Shang, et al. Solvothermal synthesis of novel magnetic nickel based iron oxide nanocomposites for selective capture of global- and monophosphopeptides. *Analytical Chemistry*, Vol. 92, No. 1, 2019, pp. 1058–1067.

[37] Meftah, A. M., E. Gharibshahi, N. Soltani, W. Yunus, and E. Saion. Structural, optical and electrical properties of PVA/PANI/nickel nanocomposites synthesized by gamma radiolytic method. *Polymers*, Vol. 6, No. 9, 2014, pp. 2435–2450.

[38] Diva, T. N., K. Zare, F. Taleshi, and M. Yousefi. Synthesis, characterization, and application of nickel oxide/CNT nanocomposites to remove Pb^{2+} from aqueous solution. *Journal of Nanostructure in Chemistry*, Vol. 7, No. 3, 2017, pp. 273–281.

[39] Neiva, E. G., M. M. Oliveira, M. F. Bergamini, L. H. Marcolino, and A. J. Zarbin. One material, multiple functions: graphene/$Ni(OH)_2$ thin films applied in batteries, electrochromism and sensors. *Scientific Reports*, Vol. 6, No. 1, 2016, pp. 1–14.

[40] Ji, Z., X. Shen, G. Zhu, H. Zhou, and A. Yuan. Reduced graphene oxide/nickel nanocomposites: facile synthesis, magnetic and catalytic properties. *Journal of Materials Chemistry*, Vol. 22, No. 8, 2012, pp. 3471–3477.

[41] Aframehr, W. M., B. Molki, R. Bagheri, P. Heidarian, and S. M. Davodi. Characterization and enhancement of the gas separation properties of mixed matrix membranes: polyimide with nickel oxide nanoparticles. *Chemical Engineering Research and Design*, Vol. 153, 2020, pp. 789–805.

[42] Wu, P.-Y., C.-H. Lin, and C.-M. Chen. Study of surface metallization of polyimide film and interfacial characterization. *Metals*, Vol. 7, No. 6, 2017, pp. 189–201.

[43] Othman, M. B. H., H. M. Akil, H. Osman, A. Khan, and Z. Ahmad. Synthesis, characterisation and thermal properties of hyperbranched polyimide derived from melamine *via* emulsion polymerisation. *Journal of Thermal Analysis and Calorimetry*, Vol. 120, No. 3, 2015, pp. 1785–1798.

[44] Mu, S., D. Wu, Y. Wang, Z. Wu, X. Yang, and W. Yang. Fabrication of nickel oxide nanocomposite layer on a flexible polyimide substrate *via* ion exchange technique. *ACS Applied Materials & Interfaces*, Vol. 2, No. 1, 2010, pp. 111–118.

[45] Othman, M. B. H., R. Ramli, Z. Mohamad Ariff, H. Md Akil, and Z. Ahmad. Thermal properties of polyimide system containing silicone segments. *Journal of Thermal Analysis and Calorimetry*, Vol. 109, No. 3, 2011, pp. 1515–1523.

[46] Yao, B., W. Hong, T. Chen, Z. Han, X. Xu, R. Hu, et al. Highly stretchable polymer composite with strain-enhanced electromagnetic interference shielding effectiveness. *Advanced Materials*, Vol. 32, No. 14, 2020, pp. 1907499–1907520.

[47] Wang, Y., S. Wu, Q. Yin, B. Jiang, and S. Mo. Data on flexibility and thermal stability of polypyrrole-based ternary nanocomposite films. *Data in Brief*, Vol. 34, 2021, pp. 106754–106760.

[48] Song, H., B. G. Kim, Y. S. Kim, Y. S. Bae, J. Kim, and Y. Yoo. Synergistic effects of various ceramic fillers on thermally conductive polyimide composite films and their model predictions. *Polymers*, Vol. 11, No. 3, 2019, pp. 484–493.

[49] Thang, V., D. Hui, J. Zhou, and P. W. Marshall. Failure prevention of seafloor composite pipelines using enhanced strain-based design. *Reviews on Advanced Materials Science*, Vol. 61, No. 1, 2022, pp. 306–321.

[50] Kumar, V., R. Singh, I. Ahuja, and J. P. Davim. On nanographene-reinforced polyvinylidene fluoride composite matrix for 4D applications. *Journal of Materials Engineering and Performance*, Vol. 30, No. 7, 2021, pp. 4860–4871.

[51] Annappa, A., S. Basavarajappa, and J. P. Davim. Effect of organoclays on mechanical properties of glass fiber-reinforced epoxy nanocomposite. *Polymer Bulletin (Berlin, Germany)*, Vol. 79, No. 7, 2022, pp. 5085–5103.

[52] Yeh, S. C., J. Y. Lee, C. T. Hsieh, Y. C. Huang, K. S. Wang, C. H. Wu, et al. Synthesis and properties of cyclopentyl cardo-type polyimides based on dicyclopentadiene. *Polymers*, Vol. 11, No. 12, 2019, pp. 2029–2044.

[53] Huang, H., C. Karlsson, M. Stromme, A. Gogoll, and M. Sjodin. Synthesis and characterization of poly-3-((2,5-hydroquinone) vinyl)-1H-pyrrole: investigation on backbone/pendant interactions in a conducting redox polymer. *Physical Chemistry Chemical Physics*, Vol. 19, No. 16, 2017, pp. 10427–10435.

[54] Li, F., J. Liu, X. Liu, Y. Wang, X. Gao, X. Meng, et al. High performance soluble polyimides from ladder-type fluorinated dianhydride with polymorphism. *Polymers*, Vol. 10, No. 5, 2018, pp. 546–563.

[55] Susa, A., J. Bijleveld, M. Hernandez Santana, and S. J. Garcia. Understanding the effect of the dianhydride structure on the properties of semiaromatic polyimides containing a biobased fatty diamine. *ACS Sustainable Chemistry & Engineering*, Vol. 6, No. 1, 2018, pp. 668–678.

[56] Othman, M. B. H., Z. Ahmad, H. Osman, M. F. Omar, and H. M. Akil. Thermal degradation behavior of a flame retardant melamine derivative hyperbranched polyimide with different terminal groups. *RSC Advances*, Vol. 5, No. 122, 2015, pp. 92664–92676.

[57] Rusli, A., M. H. Othman, and K. K. Marsilla. Plast high Heat resis app. *Plastics & Polymers*, Vol. 4, 2021, pp. 200–215.

[58] Pan, Z., S. Han, J. Wang, S. Qi, G. Tian, and D. Wu. Polyimide fabric-reinforced polyimide matrix composites with excellent thermal, mechanical, and dielectric properties. *High Performance Polymers*, Vol. 32, No. 10, 2020, pp. 1085–1093.

[59] Utracki, L. History of commercial polymer alloys and blends (from a perspective of the patent literature). *Polymer Engineering & Science*, Vol. 35, No. 1, 1995, pp. 2–17.

[60] Gouda, K., S. Bhowmik, and B. Das. A review on allotropes of carbon and natural filler-reinforced thermomechanical properties of upgraded epoxy hybrid composite. *Reviews on Advanced Materials Science*, Vol. 60, No. 1, 2021, pp. 237–275.

[61] Gouzman, I., E. Grossman, R. Verker, N. Atar, A. Bolker, and N. Eliaz. Advances in polyimide-based materials for space applications. *Advanced Materials*, Vol. 31, No. 8, 2019, id. 1807738.

[62] Yoonessi, M., J. R. Gaier, J. A. Peck, and M. A. Meador. Controlled direction of electrical and mechanical properties in nickel tethered graphene polyimide nanocomposites using magnetic field. *Carbon*, Vol. 84, 2015, pp. 375–382.

[63] Tambrallimath, V., R. Keshavamurthy, P. Davim, G. P. Kumar, G. Pignatta, A. Badari, et al. Synthesis and characterization of flyash reinforced polymer composites developed by fused filament fabrication. *Journal of Materials Research and Technology*, Vol. 21, 2022, pp. 810–826.

[64] Fujioka, D., S. Ikeda, K. Akamatsu, H. Nawafune, and K. Kojima. Preparation of Ni nanoparticles by liquid-phase reduction to fabricate metal nanoparticle–polyimide composite films. *RSC Advances*, Vol. 9, No. 12, 2019, pp. 6438–6443.

[65] Loeblein, M., A. Bolker, S. H. Tsang, N. Atar, C. Uzan-Saguy, R. Verker, et al. 3D graphene-infused polyimide with enhanced electrothermal performance for long-term flexible space applications. *Small*, Vol. 11, No. 48, 2015, pp. 6425–6434.

[66] Ding, X., W. Wang, Y. Wang, R. Xu, and D. Yu. High-performance flexible electromagnetic shielding polyimide fabric prepared by nickel–tungsten–phosphorus electroless plating. *Journal of Alloys and Compounds*, Vol. 777, 2019, pp. 1265–1273.

[67] Okafor, P. and J. Iroh. Electrochemical properties of porous graphene/polyimide–nickel oxide hybrid composite electrode material. *Energies*, Vol. 14, No. 3, 2021, pp. 582–599.

[68] Priyadarshini, B. G., S. Aich, and M. Chakraborty. On the microstructure and interfacial properties of sputtered nickel thin film on Si (1 0 0). *Bulletin of Materials Science*, Vol. 37, No. 6, 2014, pp. 1265–1273.

[69] Huang, S.-E., F.-Y. Shen, and W.-P. Dow. Polyimide metallization using nickel nano-film as both catalyst and barrier layer of copper electroless deposition. *Journal of the Electrochemical Society*, Vol. 166, No. 15, 2019, pp. 843–850.

[70] Matsumura, Y., Y. Enomoto, T. Tsuruoka, K. Akamatsu, and H. Nawafune. Fabrication of copper damascene patterns on polyimide using direct metallization on trench templates generated by imprint lithography. *Langmuir*, Vol. 26, No. 14, 2010, pp. 12448–12454.

[71] Dorneanu, P. P., A. Airinei, M. Homocianu, and N. Olaru. Photophysical and surface characteristics of electrospun polysulfone/nickel fibers. *Materials Research Bulletin*, Vol. 64, 2015, pp. 306–311.

[72] Chang, T.-F. M., C.-C. Wang, C.-Y. Yen, S.-H. Chen, C.-Y. Chen, and M. Sone. Metallization of polyimide films with enlarged area by conducting the catalyzation in supercritical carbon dioxide. *Microelectronic Engineering*, Vol. 153, 2016, pp. 1–4.

[73] Yue, Z., W. Zhu, Y. Li, Z. Wei, N. Hu, Y. Suo, et al. Surface engineering of a nickel oxide–nickel hybrid nanoarray as a versatile catalyst for both superior water and urea oxidation. *Inorganic Chemistry*, Vol. 57, No. 8, 2018, pp. 4693–4698.

[74] Nwanya, A. C., M. M. Ndipingwi, C. O. Ikpo, R. M. Obodo, S. C. Nwanya, S. Botha, et al. Zea mays lea silk extract mediated synthesis of nickel oxide nanoparticles as positive electrode material for asymmetric supercabattery. *Journal of Alloys and Compounds*, Vol. 822, 2020, pp. 153581–153592.
[75] Zeng, Z., X. Peng, J. Zheng, and C. Xu. Heteroatom-doped nickel oxide hybrids derived from metal–organic frameworks based on novel schiff base ligands toward high-performance electrochromism. *ACS Applied Materials & Interfaces*, Vol. 13, No. 3, 2021, pp. 4133–4145.
[76] Mokoena, T. P., H. C. Swart, and D. E. Motaung. A review on recent progress of p-type nickel oxide based gas sensors: future perspectives. *Journal of Alloys and Compounds*, Vol. 805, 2019, pp. 267–294.
[77] Wang, K. H., H. Ikeuchi, M. Yoshida, T. Miura, I. P. Liu, G. Watanabe, et al. Nanometer-thick nickel oxide films prepared from alanine-chelated coordination complexes for electrochromic smart windows. *ACS Applied Nano Materials*, Vol. 3, No. 9, 2020, pp. 9528–9537.
[78] Suhasini, A. and K. V. Kumar. Investigation of polyurethane diol/polycaprolactone: nickel oxide nanocomposites. *Journal of Thermoplastic Composite Materials*, Vol. 34, No. 5, 2021, pp. 671–694.
[79] Mu, S., D. Wu, S. Qi, and Z. Wu. Preparation of polyimide/zinc oxide nanocomposite films *via* an ion-exchange technique and their photoluminescence properties. *Journal of Nanomaterials*, V`ol. 2021, No. 8, 2011, pp. 1–10.
[80] Bhat, S. A., F. Zafar, A. U. Mirza, A. H. Mondal, A. Kareem, Q. M. R. Haq, et al. NiO nanoparticle doped-PVA-MF polymer nanocomposites: preparation, Congo red dye adsorption and antibacterial activity. *Arabian Journal of Chemistry*, Vol. 13, No. 6, 2020, pp. 5724–5739.
[81] Manzoor, A., H. M. Siddiqi, and A. Shah. Development of sulphonated co-polyimide based sensor for metal ions detection in aqueous media. *Inorganic Chemistry Communications*, Vol. 146, 2022, id. 110088.
[82] Khanahmadzadeh, S. and F. Barikan. Fabrication and magnetic properties of polyimide/nickel oxide nanocomposite. *International Journal of Nano Dimensions*, Vol. 5, No. 4, 2014, pp. 365–370.
[83] Lv, Q., X. Sun, C. Zhang, Y. Liu, Q. Wang, L. Liu, et al. Porous nickel–zinc ferrite/polyaniline/polyimide composite based on improved impedance matching for electromagnetic microwave absorption. *Polymer Composites*, Vol. 43, No. 12, 2022, pp. 8737–8748.
[84] Yoonessi, M., D. A. Scheiman, M. Dittler, J. A. Peck, J. Ilavsky, J. R. Gaier, et al. High-temperature multifunctional magnetoactive nickel graphene polyimide nanocomposites. *Polymers*, Vol. 54, No. 11, 2013, pp. 2776–2784.
[85] Kośla, K., M. Olejnik, and K. Olszewska. Preparation and properties of composite materials containing graphene structures and their applicability in personal protective equipment: a review. *Reviews on Advanced Materials Science*, Vol. 59, No. 1, 2020, pp. 215–242.
[86] Yang, G., L. Li, W. B. Lee, and M. C. Ng. Structure of graphene and its disorders: a review. *Science and Technology of Advanced Materials*, Vol. 19, No. 1, 2018, pp. 613–648.
[87] Gong, J., Z. Liu, J. Yu, D. Dai, W. Dai, S. Du, et al. Graphene woven fabric-reinforced polyimide films with enhanced and anisotropic thermal conductivity. *Composites Part A: Applied Science and Manufacturing*, Vol. 87, 2016, pp. 290–296.
[88] Mercado, E., J. Anaya, and M. Kuball. Impact of polymer residue level on the in-plane thermal conductivity of suspended large-area graphene sheets. *ACS Applied Materials & Interfaces*, Vol. 13, No. 15, 2021, pp. 17910–17919.
[89] Ma, L., Z. Dou, D. Li, J. Liu, Y. Xu, and G. Wang. Facile synthesis of nitrogen-doped porous Ni@ C nanocomposites with excellent synergistically enhanced microwave absorption and thermal conductive performances. *Carbon*, Vol. 201, 2023, pp. 587–598.
[90] Akamatsu, K., K. Nakahashi, S. Ikeda, and H. Nawafune. Fabrication and structural characterization of nanocomposites consisting of Ni nanoparticles dispersed in polyimide films. *The European Physical Journal D-Atomic, Molecular, Optical and Plasma Physics*, Vol. 24, No. 1, 2003, pp. 377–380.
[91] Zhou, Y., S. Chen, D. Wu, L. Liu, H. Luo, and D. Zhang. Enhanced dielectric properties of poly (vinylidene fluoride-co-hexafluoropropylene) nanocomposites using oriented nickel nanowires. *Composites Communication*, Vol. 16, 2019, pp. 11–19.
[92] Ishida, A. and M. Sato. Ti–Ni–Cu shape-memory alloy thin film formed on polyimide substrate. *Thin Solid Films*, Vol. 516, No. 21, 2008, pp. 7836–7839.
[93] Mundil, R., S. Hermanová, M. Peschel, A. Lederer, and J. Merna. On the topology of highly branched polyethylenes prepared by amine−imine nickel and palladium complexes: the effect of ortho-aryl substituents. *Polymer International*, Vol. 67, No. 7, 2018, pp. 946–956.
[94] Vokoun, D., P. Sysel, L. Heller, L. Kadeřávek, M. Svatuška, T. Goryczka, et al. NiTi–polyimide composites prepared using thermal imidization process. *Journal of Materials Engineering and Performance*, Vol. 25, No. 5, 2016, pp. 1993–1999.
[95] Mundil, R., A. Sokolohorskyj, J. Hošek, J. Cvačka, I. Císařová, J. Kvíčala, et al. Nickel and palladium complexes with fluorinated alkyl substituted α-diimine ligands for living/controlled olefin polymerization. *Polymer Chemistry*, Vol. 9, No. 10, 2018, pp. 1234–1248.
[96] Kislenko, V. and L. Oliynyk. Complex formation of polyethyleneimine with copper(II), nickel(II), and cobalt(II) ions. *Journal of Polymer Science Part A: Polymer Chemistry*, Vol. 40, No. 7, 2002, pp. 914–922.
[97] Anandhan, S. and S. Bandyopadhyay. Polymer nanocomposites: from synthesis to applications. *Nanocomposites and Polymers with Analytical Methods*, Vol. 1, No. 1, 2011, pp. 1–28.
[98] Veeralingam, S. and S. Badhulika. Two-dimensional metallic $NiSe_2$ nanoclusters-based low-cost, flexible, amperometric sensor for detection of neurological drug carbamazepine in human sweat samples. *Frontiers in Chemistry*, Vol. 8, 2020, pp. 337–346.
[99] Thévenot, J., H. Oliveira, O. Sandre, and S. Lecommandoux. Magnetic responsive polymer composite materials. *Chemical Society Reviews*, Vol. 42, No. 17, 2013, pp. 7099–7116.
[100] Zhou, Y., L. Zhao, N. Zhang, C. Chang, Z. Song, W. An, et al. Self-assembled growing ultrathin Ag@ NiO core–shell nanowires for stable freestanding transparent conductive colorless polyimide nanomembranes. *Journal of Alloys and Compounds*, Vol. 935, No. 2, 2022, id. 168012.
[101] Zhang, L., C. Shi, K. Y. Rhee, and N. Zhao. Properties of $Co_{0.5}Ni_{0.5}Fe_2O_4$/carbon nanotubes/polyimide nanocomposites for microwave absorption. *Composites Part A: Applied Science and Manufacturing*, Vol. 43, No. 12, 2012, pp. 2241–2248.

[102] Zhang, J., M. B. Sullivan, J. W. Zheng, K. P. Loh, and P. Wu. Theoretical study on polyimide−Cu (100)/Ni (100) adhesion. *Chemistry of Materials*, Vol. 18, No. 22, 2006, pp. 5312–5316.

[103] Sribala, G., B. Meenarathi, and R. Anbarasan. Synthesis, characterization, and catalytic activity of fluorescent polyimide nanocomposites. *Journal of Applied Polymer Science*, Vol. 134, 2017, pp. 44633–44644.

[104] Sugimoto, T., Y. Atsumi, M. Kono, M. Kikuta, E. Ishiko, M. Yamagata, et al. Application of bis (fluorosulfonyl) imide-based ionic liquid electrolyte to silicon–nickel–carbon composite anode for lithium-ion batteries. *Journal of Power Sources*, Vol. 195, No. 18, 2010, pp. 6153–6156.

[105] Gao, W., Z. Zhang, Y. Zhang, B. Ma, J. Luo, J. Deng, et al. Efficient carbon nanotube/polyimide composites exhibiting tunable temperature coefficient of resistance for multi-role thermal films. *Composites Science and Technology*, Vol. 199, 2020, pp. 108333–108343.

[106] Luo, Y., Q. Chen, D. Zhu, and M. Matsuo. Graphite carbon foam films prepared from porous polyimide with in situ formed catalytic nickel particles. *Journal of Applied Polymer Science*, Vol. 116, No. 4, 2010, pp. 2110–2118.

[107] Bumai, Y. A., N. I. Dolgikh, A. A. Kharchenko, V. F. Valeev, V. I. Nuzhdin, R. I. Khaibullin, et al. Optical properties of polyimide films implanted with Ni^+ ions. *Journal of Applied Spectroscopy*, Vol. 81, No. 2, 2014, pp. 188–192.

[108] Jum'h, I., A. Telfah, M. S. Mousa, M. J. A. Ahmad, C. J. Tavares, and R. Hergenröder. XPS, UV–Vis, XRD, and PL spectroscopies for studying nickel nanoparticle positioning effect on nanocomposite film properties. *Journal of Applied Polymer Science*, Vol. 139, No. 26, 2022, id. 52433.

[109] Sun, B., P. Wang, B. Ma, J. Deng, and J. Luo. Effects of annealing on the temperature coefficient of resistance of nickel film deposited on polyimide substrate. *Vaccum*, Vol. 160, 2019, pp. 18–24.

[110] Othman, M. B. H., Z. Ahmad, H. M. Akil, M. R. Zakaria, and F. Ullah. The effects of the SiOSi segment presence in BAPP/BPDA polyimide system on morphology and hardness properties for optoelectronic application. *Material and Design*, Vol. 82, 2015, pp. 98–105.

[111] Ashfaq, A., M. C. Clochard, X. Coqueret, C. Dispenza, M. S. Driscoll, P. Ulański, et al. Polymerization reactions and modifications of polymers by ionizing radiation. *Polymers*, Vol. 12, No. 12, 2020, pp. 2877–2944.

[112] Flores-Rojas, G., F. López-Saucedo, and E. Bucio. Gamma-irradiation applied in the synthesis of metallic and organic nanoparticles: a short review. *Radiation Physics and Chemistry*, Vol. 169, 2020, pp. 107962–108009.

[113] Tamai, T., M. Watanabe, Y. Kobayashi, J. Kobata, Y. Nakahara, and S. Yajima. Surface modification of polyethylene naphthalate substrates by ultraviolet light-irradiation and assembling multilayers and their application in electroless deposition: the chemical and physical properties of the stratified structure. *Colloids and Surfaces A: Physicochemical and Engineering Aspects*, Vol. 575, 2019, pp. 230–236.

[114] Zhang, Y., H. L. Ma, K. Cao, L. Wang, X. Zeng, X. Zhang, et al. Gamma irradiation-induced preparation of graphene–Ni nanocomposites with efficient electromagnetic wave absorption. *Materials*, Vol. 11, No. 11, 2018, pp. 2145–2155.

[115] Park, S.-J., J. Eden, K. Jain, and M. Klosner. Flexible arrays of Ni/polyimide/Cu microplasma devices with a dielectric barrier and excimer laser ablated microcavities. *Japanese Journal of Applied Physics*, Vol. 45, No. 10S, 2006, pp. 8221–8224.

[116] Hsiao, S.-H. and Y.-J. Chen. Structure–property study of polyimides derived from PMDA and BPDA dianhydrides with structurally different diamines. *European Polymer Journal*, Vol. 38, No. 4, 2002, pp. 815–828.

[117] Qi, H., G. Li, G. Liu, C. Zhang, G. Zhang, T. Wang, et al. Comparative study on tribological mechanisms of polyimide composites when sliding against medium carbon steel and NiCrBSi. *Journal of Colloid and Interface Science*, Vol. 506, 2017, pp. 415–428.

[118] Reinspach, J., M. Lindblom, O. von Hofsten, M. Bertilson, H. M. Hertz, and A. Holmberg. Cold-developed electron-beam-patterned ZEP 7000 for fabrication of 13 nm nickel zone plates. *Journal of Vacuum Science & Technology B: Microelectronics and Nanometer Structures Processing, Measurement, and Phenomena*, Vol. 27, No. 6, 2009, pp. 2593–2596.

[119] Romand, M., M., Charbonnier, and Y. Goepfert. Plasma and VUV pretreatments of polymer surfaces for adhesion promotion of electroless Ni or Cu films. *Journal of Adhesion and Interface*, Vol. 4, No. 2, 2003, pp. 10–20.

[120] Chang, Y.-T., K.-Y. Hung, H.-T. Young, K.-M. Li, and R. K. Chen. Aerosol jet printing of nickel oxide nanoparticle ink with ultraviolet radiation curing for thin-film temperature sensors. *The International Journal of Advanced Manufacturing Technology*, Vol. 118, No. 5, 2021, pp. 1–9.

[121] Das, L., J. C. Poutsma, and M. J. Kelley. Effect of 172-nm UV irradiation on polyimide and its application in surface modification by grafting. *High Performance Polymers*, Vol. 32, No. 7, 2020, pp. 761–774.

[122] Adnan, M. M., A. R. M. Dalod, M. H. Balci, J. Glaum, and M. A. Einarsrud. *In situ* synthesis of hybrid inorganic(-)polymer nanocomposites. *Polymers*, Vol. 10, No. 10, 2018, pp. 1129–1161.

[123] Hu, N., L. Wei, Y. Wang, R. Gao, J. Chai, Z. Yang, et al. Graphene oxide reinforced polyimide nanocomposites *via* in situ polymerization. *Journal of Nanoscience and Nanotechnology*, Vol. 12, No. 1, 2012, pp. 173–178.

[124] Pham-Truong, T. N., O. Mebarki, C. Ranjan, H. Randriamahazaka, and J. Ghilane. Electrochemical growth of metallic nanoparticles onto immobilized polymer brush ionic liquid as a hybrid electrocatalyst for the hydrogen evolution reaction. *ACS Applied Materials & Interfaces*, Vol. 11, No. 4, 2019, pp. 38265–38275.

[125] Ramesh, G., S. Porel, and T. Radhakrishnan. Polymer thin films embedded with in situ grown metal nanoparticles. *Chemical Society Reviews*, Vol. 38, No. 9, 2009, pp. 2646–2656.

[126] Zhang, X., J. He, and B. Jin. In situ nanopressing: a general approach to robust nanoparticles-polymer surface structures. *Scientific Reports*, Vol. 6, No. 1, 2016, pp. 1–6.

[127] Dai, D., H. Wang, C. Li, X. Qin, and T. Li. A physical entangling strategy for simultaneous interior and exterior modification of metal-organic framework with polymers. *Angewandte Chemie*, Vol. 133, No. 13, 2020, pp. 7465–7472.

[128] Merabtine, S., F. Zighem, D. Faurie, A. Garcia-Sanchez, P. Lupo, and A. O. Adeyeye. Multicracking and magnetic behavior of $Ni_{80}Fe_{20}$ nanowires deposited onto a polymer substrate. *Nano Letters*, Vol. 18, No. 5, 2018, pp. 3199–3202.

[129] Faurie, D., F. Zighem, P. Godard, G. Parry, T. Sadat, D. Thiaudière, et al. In situ X-ray diffraction analysis of 2D crack patterning in thin films. *Acta Materialia*, Vol. 165, 2019, pp. 177–182.

[130] Zhao, M. Q., Q. Zhang, X. L. Jia, J. Q. Huang, Y. H. Zhang, and F. Wei. Hierarchical composites of single/double-walled carbon nanotubes interlinked flakes from direct carbon deposition on layered double hydroxides. *Advanced Functional Materials*, Vol. 20, No. 4, 2010, pp. 677–685.

[131] Wang, T., X. Li, Y. Jiang, Y. Zhou, L. Jia, and C. Wang. Reduced graphene oxide-polyimide/carbon nanotube film decorated with NiSe nanoparticles for electrocatalytic hydrogen evolution reactions. *Electrochimica Acta*, Vol. 243, 2017, pp. 291–298.

[132] Ding, Q., M. Liu, Y.-E. Miao, Y. Huang, and T. Liu. Electrospun nickel-decorated carbon nanofiber membranes as efficient electrocatalysts for hydrogen evolution reaction. *Electrochimica Acta*, Vol. 159, 2015, pp. 1–7.

[133] Chen, J. J., Q. An, R. D. Rodriguez, E. Sheremet, Y. Wang, E. Sowade, et al. Surface modification with special morphology for the metallization of polyimide film. *Applied Surface Science*, Vol. 487, 2019, pp. 503–509.

[134] Schrittwieser, S., D. Reichinger, and J. Schotter. Applications, surface modification and functionalization of nickel nanorods. *Materials*, Vol. 11, No. 1, 2017, pp. 45–73.

[135] Liu, Y., Q. Chen, and X. Du. Effect of direct fluorination on surface and electrical properties of polyimide thin films. *Materials Letters*, Vol. 223, 2018, pp. 207–209.

[136] Liu, T.-J., C.-H. Chen, P.-Y. Wu, C.-H. Lin, and C.-M. Chen. Efficient and adhesiveless metallization of flexible polyimide by functional grafting of carboxylic acid groups. *Langmuir*, Vol. 35, No. 22, 2019, pp. 7212–7221.

[137] Miyauchi, K., H. Watanabe, and M. Yuasa. A study of adhesive improvement of a Cr–Ni alloy layer on a liquid crystal polymer (LCP) surface. *Progress in Organic Coatings*, Vol. 94, 2016, pp. 73–78.

[138] Park, J. W., A. V. Takaloo, S. H. Kim, K. R. Son, D. Y. Kang, S. K. Kang, et al. Surface-modified ultra-thin indium zinc oxide films with tunable work function for efficient hole transport in flexible indoor organic photovoltaics. *Journal of Power Sources*, Vol. 489, 2021, pp. 29507–229518.

[139] Li, L., Y. Ma, G. Gao, H. Wang, X. Yang, J. Xie, et al. Pretreatment and deposition process of electroless Ni plating on polyimide film for electronic field applications. *Colloids and Surfaces A: Physicochemical and Engineering Aspects*, Vol. 477, 2015, pp. 42–48.

[140] Tomita, S., P. E. Jönsson, K. Akamatsu, H. Nawafune, and H. Takayama. Controlled magnetic properties of Ni nanoparticles embedded in polyimide films. *Physical Review B*, Vol. 76, No. 17, 2007, pp. 174432–174438.

[141] Cherng, S.-J., C.-M. Chen, W.-P. Dow, C.-H. Lin, and S.-W. Chen. Chemical deposition of Ni/Pt Bi-layer on polyimide film as flexible counterelectrodes for dye-sensitized solar cells. *Electrochemical and Solid-State Letters*, Vol. 14, No. 7, 2011, pp. 13–15.

[142] Noh, B.-I., J.-W. Yoon, and S.-B. Jung. Fabrication and adhesion strength of Cu/Ni–Cr/polyimide films for flexible printed circuits. *Microelectronic Engineering*, Vol. 88, No. 6, 2011, pp. 1024–1027.

[143] Min, K.-J., S.-C. Park, K. H. Lee, Y. Jeong, and Y.-B. Park. Interfacial adhesion characteristics between electroless-plated Ni and polyimide films modified by alkali surface pretreatment. *Journal of Electronic Materials*, Vol. 38, No. 12, 2009, pp. 2455–2460.

[144] Cen-Puc, M., A. Schander, M. G. Vargas Gleason, and W. Lang. An assessment of surface treatments for adhesion of polyimide thin films. *Polymers*, Vol. 13, No. 12, 2021, pp. 1955–1969.

[145] Wang, Z., L. Qin, Q. Chen, W. Yang, and H. Qu. Flexible UWB antenna fabricated on polyimide substrate by surface modification and in situ self-metallization technique. *Microelectronic Engineering*, Vol. 206, 2019, pp. 12–16.

[146] Gu, Y. and J. F. Federici. Fabrication of a flexible current collector for lithium ion batteries by inkjet printing. *Batteries*, Vol. 4, No. 3, 2018, pp. 42–53.

[147] Chae, C., J. H. Han, S. S. Lee, Y. Choi, T. H. Kim, and S. Jeong. A printable metallic current collector for all-printed high-voltage micro-supercapacitors: instantaneous surface passivation by flash-light-sintering reaction. *Advanced Functional Materials*, Vol. 30, No. 25, 2020, pp. 2000715–2000726.

[148] Liu, T.-J., M. C. Sil, and C.-M. Chen. Well-organized organosilane composites for adhesion enhancement of heterojunctions. *Composites Science and Technology*, Vol. 193, 2020, pp. 108135–108146.

[149] Woo, T.-G., I.-S. Park, K.-H. Jung, W.-Y. Jeon, and K.-W. Seol. Effect of N_2 plasma treatment on the adhesion of Cu/Ni thin film to polyimide. *Metals and Materials International*, Vol. 17, No. 5, 2011, pp. 789–795.

[150] Huang, C.-C., Z.-K. Kao, and Y.-C. Liao. Flexible miniaturized nickel oxide thermistor arrays *via* inkjet printing technology. *ACS Applied Materials & Interfaces*, Vol. 5, No. 24, 2013, pp. 12954–12959.

[151] Khan, Y., M. Garg, Q. Gui, M. Schadt, A. Gaikwad, D. Han, et al. Flexible hybrid electronics: direct interfacing of soft and hard electronics for wearable health monitoring. *Advanced Functional Materials*, Vol. 26, No. 47, 2016, pp. 8764–8775.

[152] Behroozfar, A., M. E. Hossain Bhuiyan, S. Daryadel, D. Edwards, B. J. Rodriguez, and M. Minary-Jolandan. Additive printing of pure nanocrystalline nickel thin films using room environment electroplating. *Nanotechnology*, Vol. 31, No. 5, 2020, pp. 55301–55310.

[153] Cai, J., C. Lv, and A. Watanabe. Laser direct writing and selective metallization of metallic circuits for integrated wireless devices. *ACS Applied Materials & Interfaces*, Vol. 10, No. 1, 2018, pp. 915–924.

[154] Li, G., X. Mo, W.-C. Law, and K. C. Chan. 3D printed graphene/nickel electrodes for high areal capacitance electrochemical storage. *Journal of Materials Chemistry A: Materials for Energy and Sustainability*, Vol. 7, No. 8, 2019, pp. 4055–4062.

[155] Kotnur, V., F. Tichelaar, and G. Janssen. Sputter deposited Ni–Ti thin films on polyimide substrate. *Surface and Coatings Technology*, Vol. 222, 2013, pp. 44–47.

[156] Ye, J., R. K. Mishra, A. R. Pelton, and A. M. Minor. Direct observation of the NiTi martensitic phase transformation in nanoscale volumes. *Acta Materialia*, Vol. 58, No. 2, 2010, pp. 490–498.

[157] Wang, J.-J., H. Hu, and C.-H. Shang. Effect of annealing on the performance of nickel thermistor on polyimide substrate. *Thin Solid Films*, Vol. 632, 2017, pp. 28–34.

[158] Woo, T.-G., I.-S. Park, K.-H. Jung, W.-Y. Jeon, and K.-W. Seol. Effect of RF sputtering power on the adhesion of Ni thin film to polyimide. *Electronic Materials Letters*, Vol. 7, No. 4, 2011, pp. 353–358.

[159] Ishida, A. Ti–Ni–Cu/polyimide composite-film actuator and simulation tool. *Sensors and Actuators A: Physical*, Vol. 222, 2015, pp. 228–236.

[160] Mohri, M. and M. Nili-Ahmadabadi. On the nano-glass formation of the Ni–Ti thin films and related micro-structure and mechanical properties by controlling sputtering conditions. *Materials Research Express*, Vol. 6, No. 7, 2019, pp. 76421–76442.

[161] Reddy, B. P., K. S. Ganesh, S.-H. Park, and O. Hussain. RF-sputter deposited flexible copper oxide thin films for electrochemical energy storage. *Indian Journal of Physics and Proceedings of the Indian Association for the Cultivation of Science*, Vol. 92, No. 1, 2018, pp. 21–27.

[162] Jayachandran, S., K. Akash, S. M. Prabu, M. Manikandan, M. Muralidharan, A. Brolin, et al. Investigations on performance viability of NiTi, NiTiCu, CuAlNi and CuAlNiMn shape memory alloy/Kapton composite thin film for actuator application. *Composites Part B: Engineering*, Vol. 176, 2019, pp. 107182–107192.
[163] Catauro, M. and S. V. Ciprioti. Characterization of hybrid materials prepared by sol-gel method for biomedical implementations. A critical review. *Materials*, Vol. 14, No. 7, 2021, pp. 1788–1811.
[164] Tan, W. K., H. Muto, G. Kawamura, Z. Lockman, and A. Matsuda. Nanomaterial fabrication through the modification of sol–gel derived coatings. *Nanomaterials*, Vol. 11, No. 1, 2021, pp. 181–211.
[165] Nardi, M. V., M. Timpel, G. Ligorio, N. Zorn Morales, A. Chiappini, T. Toccoli, et al. Versatile and scalable strategy to grow sol–gel derived 2H-MoS_2 thin films with superior electronic properties: a memristive case. *ACS Applied Materials & Interfaces*, Vol. 10, No. 40, 2018, pp. 34392–34400.
[166] Dojcinovic, M. P., Z. Z. Vasiljevic, J. Kovac, N. B. Tadic, and M. V. Nikolic. Nickel manganite–sodium alginate nano-biocomposite for temperature sensing. *Chemosensors*, Vol. 9, No. 9, 2021, id. 241.
[167] He, J., J. Zhang, S. Qian, X. Chen, J. Qian, X. Hou, et al. Flexible heterogeneous integration of PZT film by controlled spalling technology. *Journal of Alloys and Compounds*, Vol. 807, 2019, pp. 151696–151703.
[168] He, Y., Y. Li, J. Zhang, S. Wang, D. Huang, G. Yang, et al. Low-temperature strategy toward Ni-NC@ Ni core–shell nanostructure with single-Ni sites for efficient CO_2 electroreduction. *Nano Energy*, Vol. 77, 2020, pp. 105010–105018.
[169] Zhang, Y., W. Fan, H. Lu, and T. Liu. Highly porous polyimide-derived carbon aerogel as advanced three-dimensional framework of electrode materials for high-performance supercapacitors. *Electrochimica Acta*, Vol. 283, 2018, pp. 1763–1772.
[170] Kaliyappan, K., G. Li, L. Yang, Z. Bai, and Z. Chen. An ion conductive polyimide encapsulation: new insight and significant performance enhancement of sodium based P2 layered cathodes. *Energy Storage Materials*, Vol. 22, 2019, pp. 168–178.
[171] Matsumura, Y., Y. Enomoto, T. Jyo, K. Akamatsu, and H. Nawafune. Formation of metal thin nanocomposite layer from precursor polyimide containing metal complex. *Transactions of the Materials Research Society of Japan*, Vol. 33, No. 4, 2008, pp. 1333–1336.
[172] Zhang, Y. F., S. N. Chen, W. Q. Yan, Q. Li, L. Chen, Y. X. Ou, et al. Protection of Kapton from atomic oxygen attack by SiO_x/NiCr coating. *Surface and Coatings Technology*, Vol. 423, 2021, pp. 127582–127594.
[173] Othman, M. B., M. R. Ramli, L. Y. Tyng, Z. Ahmad, and H. M. Akil. Dielectric constant and refractive index of poly (siloxane–imide) block copolymer. *Material and Design*, Vol. 32, No. 6, 2011, pp. 3173–3182.
[174] Xu, L., G. Chen, W. Wang, L. Li, and X. Fang. A facile assembly of polyimide/graphene core–shell structured nanocomposites with both high electrical and thermal conductivities. *Composites Part A: Applied Science and Manufacturing*, Vol. 84, 2016, pp. 472–481.
[175] Mi, Z., Z. Liu, J. Yao, C. Wang, C. Zhou, D. Wang, et al. Transparent and soluble polyimide films from 1,4:3,6-dianhydro-D-mannitol based dianhydride and diamines containing aromatic and semi-aromatic units: preparation, characterization, thermal and mechanical properties. *Polymer Degradation and Stability*, Vol. 151, 2018, pp. 80–89.
[176] Kaviyarasu, K., E. Manikandan, J. Kennedy, M. Jayachandran, R. Ladchumananandasiivam, U. U. De Gomes, et al. Synthesis and characterization studies of NiO nanorods for enhancing solar cell efficiency using photon upconversion materials. *Ceramics International*, Vol. 42, No. 7, 2016, pp. 8385–8394.
[177] Sreethawong, T., Y. Suzuki, and S. Yoshikawa. Photocatalytic evolution of hydrogen over mesoporous TiO_2 supported NiO photocatalyst prepared by single-step sol–gel process with surfactant template. *International Journal of Hydrogen Energy*, Vol. 30, No. 10, 2005, pp. 1053–1062.
[178] Levytskyi, V., A. Masyuk, D. Katruk, R. Kuzioła, M. Bratychak Jr, N. Chopyk, et al. Influence of polymer-silicate nucleator on the structure and properties of polyamide 6. *Chemistry*, Vol. 14, No. 4, 2020, pp. 496–503.
[179] Song, X., B. Gan, S. Qi, H. Guo, C. Y. Tang, Y. Zhou, et al. Intrinsic nanoscale structure of thin film composite polyamide membranes: connectivity, defects, and structure–property correlation. *Environment Science and Technology*, Vol. 54, No. 6, 2020, pp. 3559–3569.
[180] Deeraj, B., R. Harikrishnan, J. S. Jayan, A. Saritha, and K. Joseph. Enhanced visco-elastic and rheological behavior of epoxy composites reinforced with polyimide nanofiber. *Nano-Struct Nano-Objects*, Vol. 21, 2020, pp. 100421–100429.
[181] Ren, Y., R. Rao, S. Bhusal, V. Varshney, G. Kedziora, R. Wheeler, et al. Hierarchical assembly of gold nanoparticles on graphene nanoplatelets by spontaneous reduction: implications for smart composites and biosensing. *ACS Applied Nano Materials*, Vol. 3, No. 9, 2020, pp. 8753–8762.
[182] Motamedi, P., K. Bosnick, K. Cui, K. Cadien, and J. D. Hogan. Growth and characterization of metastable hexagonal nickel thin films *via* plasma-enhanced atomic layer deposition. *ACS Applied Materials & Interfaces*, Vol. 9, No. 29, 2017, pp. 24722–24730.
[183] Zhou, Y., D. Hui, Y. Wang, and M. Fan. Nanomechanical and dynamic mechanical properties of rubber–wood–plastic composites. *Nanotechnology Reviews*, Vol. 11, No. 1, 2022, pp. 167–175.
[184] Jang, W., J. Seo, C. Lee, S. H. Paek, and H. Han. Residual stress and mechanical properties of polyimide thin films. *Journal of Applied Polymer Science*, Vol. 113, No. 2, 2009, pp. 976–983.
[185] Mohri, M., M. Nili-Ahmadabadi, M. PouryazdanPanah, and H. Hahn. Evaluation of structure and mechanical properties of Ni-rich NiTi/Kapton composite film. *Materials Science and Engineering: A*, Vol. 668, 2016, pp. 13–19.
[186] Zhang, S., Y. Liang, X. Qian, D. Hui, and K. Sheng. Pyrolysis kinetics and mechanical properties of poly (lactic acid)/bamboo particle biocomposites: effect of particle size distribution. *Nanotechnology Reviews*, Vol. 9, No. 1, 2020, pp. 524–533.
[187] Brewster, D. A., M. D. Koch, and K. E. Knowles. Evaluation of electrochemical properties of nanostructured metal oxide electrodes immersed in redox-inactive organic media. *Physical Chemistry Chemical Physics*, Vol. 23, No. 33, 2021, pp. 17904–17916.
[188] Yin, J., J. Zhang, S. Zhang, C. Liu, X. Yu, L. Chen, et al. Flexible 3D porous graphene film decorated with nickel nanoparticles for absorption-dominated electromagnetic interference shielding. *Chemical Engineering Journal*, Vol. 421, 2021, pp. 129763–129772.
[189] Mun, J. H., H. Lee, J. U. Kim, M. Kang, A. R. Hong, H. S. Jang, et al. Magnetic property modulation of Ni thin films transferred onto flexible substrates. *Journal of Magnetism and Magnetic Materials*, Vol. 511, 2020, pp. 166968–166976.
[190] Hemmetter, A., X. Yang, Z. Wang, M. Otto, B. Uzlu, M. Andree, et al. Terahertz rectennas on flexible substrates based on one-dimensional metal-insulator-graphene diodes. *ACS Applied Electronic Materials*, Vol. 3, No. 9, 2021, pp. 3747–3753.

[191] Arjmand, T., M. Legallais, T. Haffner, M. Bawedin, C. Ternon, and B. Salem. Development of a robust fabrication process for single silicon nanowire-based omega gate transistors on polyamide substrate. *Semiconductor Science and Technology*, Vol. 36, No. 2, 2020, id. 25003.

[192] Freitas, W. J., M. H. Piazzetta, L. T. Manera, and Â. L. Gobbi. Fabrication process of integrated inductors on flexible substrate for radio frequency and microwave applications. *Journal of Vacuum Science & Technology B, Nanotechnology and Microelectronics: Materials, Processing, Measurement, and Phenomena*, Vol. 38, No. 2, 2020, pp. 23204–23210.

[193] Hasan, M. A., K. Prajwal, D. N. Sahu, A. Prasad, A. Dey, and A. Rajendra. A facile and combined methodology to fabricate sputtered thin film micro-patterns for heater/sensor applications utilizing CO_2 laser-cut masks. *Surface Engineering*, Vol. 37, No. 9, 2021, pp. 1133–1142.

[194] Zhu, Z., R. Kan, S. Hu, L. He, X. Hong, H. Tang, et al. Recent advances in high-performance microbatteries: construction, application, and perspective. *Small*, Vol. 16, No. 39, 2020, pp. 2003251–2003279.

[195] Ojstršek, A., O. Plohl, S. Gorgieva, M. Kurečič, U. Jančič, S. Hribernik, et al. Metallisation of textiles and protection of conductive layers: an overview of application techniques. *Sensors*, Vol. 21, No. 10, 2021, pp. 3508–3536.

[196] Nakonieczny, D. S., M. Antonowicz, and Z. K. Paszenda. Cenospheres and their application advantages in biomedical engineering-a systematic review. *Reviews on Advanced Materials Science*, Vol. 59, No. 1, 2020, pp. 115–130.

[197] Nag, A., S. Sapra, and S. C. Mukhopadhyay. Recent progress for nanotechnology-based flexible sensors for biomedical applications. *Handbook of Nanomaterials for Sensing Applications*, Vol. 18, 2021, pp. 379–428.

[198] Kang, J. H., Y. C. Kim, K. Cho, and C. E. Park. Effects of particle size on the molecular orientation and birefringence of magnetic nanoparticles/polyimide composites. *Journal of Applied Polymer Science*, Vol. 99, No. 6, 2006, pp. 3433–3440.

[199] Baykara, O., Ş. G. İrim, A. A. Wis, M. A. Keskin, G. Ozkoc, A. Avcı, et al. Polyimide nanocomposites in ternary structure: a novel simultaneous neutron and gamma-ray shielding material. *Polymer Advances Technology*, Vol. 31, No. 11, 2020, pp. 2466–2479.

[200] Kausar, A. Emerging polyimide and graphene derived nanocomposite foam: research and technical tendencies. *Journal of Macromolecular Science, Part A*, Vol. 58, No. 10, 2021, pp. 643–658.

[201] Zhang, D., H. Chang, P. Li, R. Liu, and Q. Xue. Fabrication and characterization of an ultrasensitive humidity sensor based on metal oxide/graphene hybrid nanocomposite. *Sensors and Actuators B: Chemical*, Vol. 225, 2016, pp. 233–240.

[202] Li, J., X. Zhang, Y. Ding, S. Zhao, Z. Ma, H. Zhang, et al. Multifunctional carbon fiber@ NiCo/polyimide films with outstanding electromagnetic interference shielding performance. *Chemical Engineering Journal*, Vol. 427, 2022, pp. 131937–131947.

[203] Qu, Z., Y. Wang, W. Wang, and D. Yu. Hierarchical $FeCoNiO_x$-PDA-rGO/WPU layers constructed on the polyimide fabric by screen printing with high microwave absorption performance. *Applied Surface Science*, Vol. 562, No. 1, 2021, pp. 150190–150200.

[204] Han, N. K., Y. C. Choi, D. U. Park, J. H. Ryu, and Y. G. Jeong. Core–shell type composites based on polyimide-derived carbon nanofibers and manganese dioxide for self-standing and binder-free supercapacitor electrode applications. *Composites Science and Technology*, Vol. 196, 2020, pp. 108212–108222.

[205] Chen, M., C. Ma, Z. Ding, L. Zhou, L. Chen, P. Gao, et al. Upgrading electrode/electrolyte interphases *via* polyamide-based quasi-solid electrolyte for long-life nickel-rich lithium metal batteries. *ACS Energy Letters*, Vol. 4, No. 4, 2021, pp. 1280–1289.

[206] Chiku, M., K. Ota, E. Higuchi, and H. Inoue. Microband-array electrode technique for the detection of reaction distributions in the depth direction of composite electrodes for the all-solid-state lithium-ion batteries. *ACS Omega*, Vol. 5, No. 27, 2020, pp. 16739–16743.

[207] Cho, Y. H., J. G. Seong, J. H. Noh, D. Y. Kim, Y. S. Chung, T. H. Ko, et al. $CoMnO_2$-decorated polyimide-based carbon fiber electrodes for wire-type asymmetric supercapacitor applications. *Molecules*, Vol. 25, No. 24, 2020, pp. 5863–5878.

[208] Wang, Q., Y. Zhang, W. Ye, and C. Wang. $Ni(OH)_2/MoS_x$ nanocomposite electrodeposited on a flexible CNT/PI membrane as an electrochemical glucose sensor: the synergistic effect of $Ni(OH)_2$ and MoS_x. *Journal of Solid State Electrochemistry*, Vol. 20, No. 1, 2016, pp. 133–142.

[209] Fang, D., B. Yan, S. Agarwal, W. Xu, Q. Zhang, S. He, et al. Electrospun poly [poly (2,5-benzophenone)] bibenzopyrrolone/polyimide nanofiber membrane for high-temperature and strong-alkali supercapacitor. *Journal of Materials Science*, Vol. 56, No. 12, 2021, pp. 9344–9355.

[210] Craton, M. T., J. D. Albrecht, P. Chahal, and J. Papapolymerou. Multimaterial aerosol jet printed magnetic nanocomposites for microwave circuits. *IEEE Transactions on Components, Packaging and Manufacturing Technology*, Vol. 11, No. 5, 2021, pp. 865–871.

[211] Chen, G., X. Chen, Y. Pan, Y. Ji, G. Liu, and W. Jin. M-gallate MOF/6FDA-polyimide mixed-matrix membranes for C_2H_4/C_2H_6 separation. *Journal of Membrane Science*, Vol. 620, 2021, id. 118852.

[212] Wang, G., Q. Chen, M. Gao, B. Yang, and D. Hui. Generalized locally-exact homogenization theory for evaluation of electric conductivity and resistance of multiphase materials. *Nanotechnology Reviews*, Vol. 9, No. 1, 2020, pp. 1–16.

[213] Yang, S., S. Liu, X. Ding, B. Zhu, J. Shi, B. Yang, et al. Permeable and washable electronics based on polyamide fibrous membrane for wearable applications. *Composites Science and Technology*, Vol. 207, 2021, id. 108729.

[214] Smith, Z. P., J. E. Bachman, T. Li, B. Gludovatz, V. A. Kusuma, T. Xu, et al. Increasing M_2(dobdc) loading in selective mixed-matrix membranes: a rubber toughening approach. *Chemistry of Materials*, Vol. 30, No. 5, 2018, pp. 1484–1495.

[215] Elbakoush, D. F. E. and D. M. Abosaf. Effect of ferrous metal on the electrical conductivity and growth of metal particles after carbonization for polyimide films. *IOSR Journal of Mechanical and Civil Engineering*, Vol. 17, No. 4, 2020, pp. 45–51.

[216] Zhang, M., L. Deng, D. Xiang, B. Cao, S. S. Hosseini, and P. Li. Approaches to suppress CO_2-induced plasticization of polyimide membranes in gas separation applications. *Process*, Vol. 7, No. 1, 2019, pp. 51–82.

[217] Chen, K., K. Xu, L. Xiang, X. Dong, Y. Han, C. Wang, L. B. Sun, et al. Enhanced CO_2/CH_4 separation performance of mixed-matrix membranes through dispersion of sorption-selective MOF nanocrystals. *Journal of Membrane Science*, Vol. 563, 2018, pp. 360–370.

[218] Othman, M. B. H., N. A. S. Ming, H. M. Akil, and Z. Ahmad. Dependence of the dielectric constant on the fluorine content and porosity of polyimides. *Journal of Applied Polymer Science*, Vol. 121, No. 6, 2011, pp. 3192–3200.

[219] Ji, D., T. Li, W. Hu, and H. Fuchs. Recent progress in aromatic polyimide dielectrics for organic electronic devices and circuits. *Advanced Materials*, Vol. 31, No. 15, 2019, id. 1806070.

[220] Wei, Y., M. Cheng, M. Wang, Q. Fu, and H. Deng. Polyimide/ $BaTiO_3$/NiNWs composites with enhanced dielectric properties. *Composites Communication*, Vol. 35, 2022, id. 101286.
[221] Padhan, A. M., S. Hajra, S. Nayak, J. Kumar, M. Sahu, H. J. Kim, et al. Triboelectrification based on NiO–Mg magnetic nanocomposite: synthesis, device fabrication, and energy harvesting performance. *Nano Energy*, Vol. 91, 2022, id. 106662.
[222] Park, S., H. Y. Chang, S. Rahimi, A. L. Lee, L. Tao, and D. Akinwande. Transparent nanoscale polyimide gate dielectric for highly flexible electronics. *Advanced Electronic Materials*, Vol. 4, No. 2, 2018, pp. 1700043–170075.
[223] Huang, X., F. Zhang, Y. Liu, and J. Leng. Active and deformable organic electronic devices based on conductive shape memory polyimide. *ACS Applied Materials & Interfaces*, Vol. 12, No. 20, 2020, pp. 23236–23243.
[224] Chang, J.-H. Equibiaxially stretchable colorless and transparent polyimides for flexible display substrates. *Reviews on Advanced Materials Science*, Vol. 59, No. 1, 2020, pp. 1–9.
[225] Jia, P., M. Lu, S. Sun, Y. Gao, R. Wang, X. Zhao, et al. Recent advances in flexible perovskite light-emitting diodes. *Advanced Materials Interfaces*, Vol. 8, No. 17, 2021, id. 2100441.
[226] Bian, Z., S. Yang, X. Zhou, and D. Hui. Band gap manipulation of viscoelastic functionally graded phononic crystal. *Nanotechnology Reviews*, Vol. 9, No. 1, 2020, pp. 515–523.
[227] Jeong, J., Q. Wang, J. Cha, D. K. Jin, D. H. Shin, S. Kwon, et al. Remote heteroepitaxy of GaN microrod heterostructures for deformable light-emitting diodes and wafer recycle. *Science Advances*, Vol. 6, No. 23, 2020, pp. 5180–5190.
[228] Liu, M., X. Pu, C. Jiang, T. Liu, X. Huang, L. Chen, et al. Large-area all-textile pressure sensors for monitoring human motion and physiological signals. *Advanced Materials*, Vol. 29, No. 41, 2017, pp. 1703700–1703709.
[229] Turkani, V. S., D. Maddipatla, B. B. Narakathu, B. N. Altay, P. D. Fleming, B. J. Bazuin, et al. Nickel based RTD fabricated *via* additive screen printing process for flexible electronics. *IEEE Access*, Vol. 7, 2019, pp. 37518–37527.
[230] Lee, K., D. Yoo, H. Oh, and G.-C. Yi. Flexible and monolithically integrated multicolor light emitting diodes using morphology-controlled GaN microstructures grown on graphene films. *Scientific Reports*, Vol. 10, No. 1, 2020, pp. 1–7.
[231] Chen, Y., S. Xie, G. Li, S. Jia, X. Gao, and X. Li. 3D nanotube-structured Ni@ MnO_2 electrodes: toward enhanced areal capacitance of planar supercapacitors. *Applied Surface Science*, Vol. 494, 2019, pp. 29–36.
[232] Mukaida, M., K. Kirihara, S. Horike, and Q. Wei. Stable organic thermoelectric devices for self-powered sensor applications. *Journal of Materials Chemistry A: Materials for Energy and Sustainability*, Vol. 8, No. 43, 2020, pp. 22544–22556.
[233] Dang, V. Q., G. S. Han, T. Q. Trung, Y. U. Jin, B. U. Hwang, H. S. Jung, et al. Methylammonium lead iodide perovskite-graphene hybrid channels in flexible broadband phototransistors. *Carbon*, Vol. 105, 2016, pp. 353–361.